[Journal of the Faculty of Science, Hokkaidô University, Japan, Ser. II, Vol. V, No. 3, 1958]

Physical Investigations on the Growth of Snow Crystals*

Ukichiro NAKAYA**, Masando HANAJIMA§
and Jiro MUGURUMA†

(Received Apr. 30, 1958)

CONTENTS

* Contract Research with Geophysics Research Directorate, Air Force Cambridge Research Center; Contract No. AF 62 (502)-1228.
** Department of Physics, Hokkaido University.
§ Transportation Technical Research Institute, Tokyo.
† Department of Geophysics, Hokkaido University.

§ 1. Introduction.

In the course of our experiments on the artificial production of snow crystals, it was observed that minute droplets of supercooled water were always existent abundantly in the air under the condition of snow crystal growth. These minute droplets do not freeze to the surface of snow crystal in a droplet form, but spread over the surface of crystal when they are attached to the surface. The so called rimed crystal is obtained only when larger droplets are formed in the atmosphere. It was supposed that the aerosol particles in the minute droplets attached to the crystal might give rise to some crystal defects and the shape of snow crystal is changed when aerosol particles are removed from the atmospheric air. In the preliminary experiment, it was observed that snow crystals developed in a needle form in the aerosol free air under the condition of dendritic growth for the ordinary air[1]. The later experiment, however, showed that this effect was due to the trace of silicone vapor which came from the flow-meter using silicone oil.

When pure air is used, the effect of removing aerosol particles is not noticed in the wide range of temperature and supersaturation. The effect was observed only in the region near the freezing point. In this region, the irregular assemblage of needles is obtained when the ordinary air is used, but it is transformed into a pseudo-dendritic shape when aerosol particles are removed. The expedition to the Mauna Loa in Hawaii Island, T. H., was undertaken in the winter of 1956–57, in order to study the shape of snow crystals observable in the region where the aerosol particles are the least. Three snowfalls were met at the summit of the Mauna Loa, 13,450 ft. altitude, and 170 microphotographs of snow crystals were taken. Almost all types of snow crystals were observed.[2] Similar experience was met in the summer of 1957 at Site 2 in Greenland, 78°N and 7,000 ft. altitude.

From these experiments it was confirmed that the minute droplets contribute to the growth of snow crystals in the way just like the gaseous condensation. The mechanism of attachment of these droplets to ice surface was studied by the method of micro-cinematography. The movie showed that the small drop which hits the ice surface does neither freeze in drop shape nor evaporate

immediately. When the surface is contaminated, the drop rolls round on the ice surface and becomes smaller and smaller while wandering, and evaporates in the time of the order of one second or half a second. When clean ice surface is used, no wandering is observed, but the droplet slides on the ice surface for a short distance, and the track is observed to remain for a few minutes.

The surface of ice has a peculiar property and the mechanism of sublimation of water vapor is also to be studied from the standpoint that the ice surface has a peculiar nature as liquid-like film. The experiment was directed towards this line, and the mechanism of sublimation was studied by the observation of the migration of fine particles scattered on the surface of snow crystal, which was caused by the evaporation of ice by sublimation. The effect of impurities in the air on the shape of snow crystals is also examined with respect to various vapors. All these results are summerized in this report.

§ 2. Snow crystals developed in aerosol free air.

a) Experimental apparatus.

In order to remove aerosol particles from the atmospheric air, a thermal impactor was used. The principle is the same as those used by former researchers in the study of nuclei in the atmosphere, but it is made larger so that the rate of air flow can be raised to 15 c.c./sec. The deatil is shown in Fig. 1. Two steel pipes are set in the concentric position. The interspace between two cylinders is 2 mm in width and 600 mm in length. The surface of each cylinder facing the gap is chromium plated. The outer cylinder is heated electrically, and the inner cylinder is cooled with running water. By the use of two thermojunctions shown in Fig. 1, the temperature difference across the gap was regulated to be 80°C. When the atmospheric air previously filtered with two cotten filters

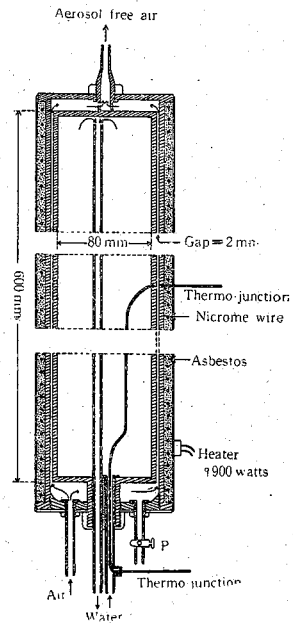

Fig. 1.
The thermal impactor.

is passed through this thermal impactor, almost all aerosol particles larger than a critical size are removed. The critical size corresponds to the expansion ratio 1.24.

The aerosol free air thus prepared is sent into the artificial snow apparatus. The apparatus is made of two concentric glass cylinders, and the principle is the same as the old apparatus used in our former investigations of artificial snow crystals, but it is developed to be air-tight in this new apparatus. All removable parts were made of ground joints. The diagram is shown in Fig. 2. The water in the reservoir R is heated electrically, and the warm vapor goes up inside of the innear tube by natural convection. The air in the apparatus is cooled from the side, and the cooled air flows down in the space between two glass cylinders. The temperature of water in the reservoir, T_w, and the temperature of the air where the crystal is made, T_a, were measured with two thermo-junctions. The air saturated with water vapor at T_w becomes supersaturated at the spot of T_a. The water vapor condenses by sublimation on a thin rabbit hair, and the snow crystal is developed in the state freely suspended in air. This artificial snow apparatus is set in a thermostat box, which is placed in the refrigerated room. The apparatus set in this thermostat box is illustrated in Photo. 7, Pl. II. T_a is the function of T_w and the ambient temperature; that is, the temperature of the thermostat box, T_r. By regulating T_r, the designated value of T_a is obtained for each of various values of T_w.

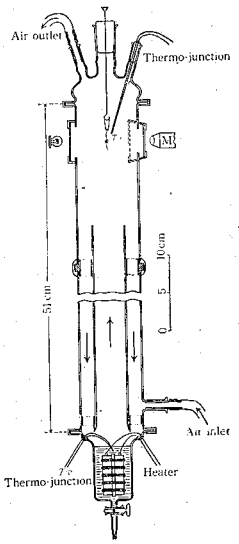

Fig. 2.
Artificial snow apparatus for using aerosol free air.

The experimental arrangement for making snow crystals in the aerosol free air is shown in Fig. 3. The atmosphric air is sent to the thermal impactor after passing two cotten filters, impurity absorber and liquid air trap. After passing the thermal impactor, the aerosol free air is sent to the expansion chamber No. 1. The expansion test is made at the beginning of a series of experiments. When no or very few fog particles are observed at the expansion

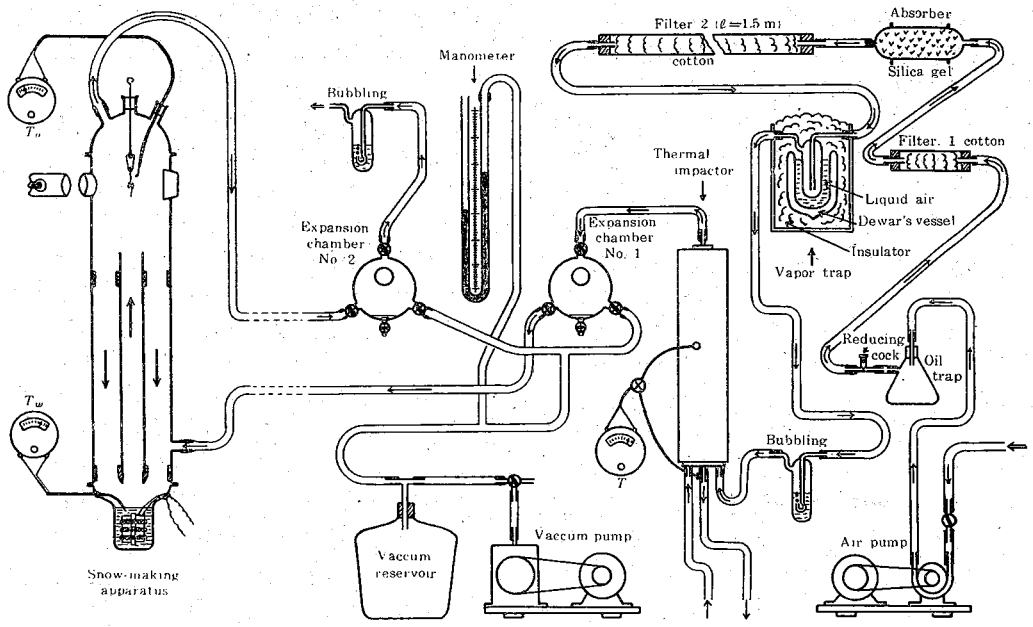

Fig. 3. Arrangement for making snow crystals in aerosol free air.

ratio of 1.23, the air is considered "aerosol free", and this air is sent into the snow making apparatus. The air comming out of the apparatus is again checked by the expansion chamber No. 2. When both expansion chambers show no or very few fog particles, the condition is considered satisfactory and the artificial snow experiment is started in the state of continuous running of this air. The expansion test is repeated occasionally during the course of a series of experiments.

b) The function of the thermal impactor.

The thermal impactor worked satisfactorily under the thermal condition of $\Delta\theta = 80°C$ across the gap of 2 mm. When the ordinary air is sent to the snow making apparatus, many fog particles appear in the upper part of the apparatus where the crystal is made. The presence of these fog particles is shown by the Tyndall scattering of light. Photo. 1, Pl. I, shows the Tyndall scattering. The thin rabbit hair is out of focus due to the long exposure of 1 sec. Under the same condition, no Tyndall scattering is observed when the air is sent after passing the cotten filters and the thermal

impactor; Photo. 2, Pl. I. In this case all aerosol particles are removed, and no fog particle can appear under the condition of snow formation.

The function of the thermal impactor is also checked by the use of the expansion chamber. Photo. 3, Pl. I, shows the mode of appearance of abundant fog particles when the ordinary air is used. The expansion ratio s is 1.23. Most of the nuclei are removed by filtering the air with two cotten filters 2 m in total length. The number of fog particles is reduced to the order of one hundredth of the former case, as shown in Photo. 4, Pl. I. Photo. 5, Pl. I, is the case when both the cotten filters and the thermal impactor are used. Very few fog particles are observed with the expansion ratio up to 1.23. When the expansion chamber shows this state, no Tyndall scattering of light is observed in the apparatus, and this state of air is called "aerosol free" in this report. This aerosol free air, however, still contains numerous minute nuclei, and many fog particles appear with the larger expansion ratio than 1.24. Photo. 6, Pl. I, shows the appearance of fog particles in the "aerosol free" air with the expansion ratio of 1.25. The nature of minute nuclei which produce fog at higher expansion ratio has been studied by many workers in this line; for example, M. VOLMER and his collaborator[3]. In this paper, however, the problem of self-nucleation or water embryo is not taken up. In the present case we are concerned to the minute droplets in the snow making apparatus, and these minute nuclei do not act as the condensation nuclei under the condition of snow formation. This is already shown in Photo. 2, Pl. I. For the present purpose, therefore, the air above mentioned, which produce no fog particle with the expansion ratio up to 1.23, may be called "aerosol free". In this paper, the term aerosol free is used in this definition.

c) Test of the new snow making appartus.

In order to confirm whether the new snow making apparatus gives the same result as our former result of the condition of snow formation, more than thirty sets of experiments were carried out under various conditions of T_a and T_w by using the ordinary air. The results are shown in Fig. 4. The curves showing the boundaries of various types of crystals are transfered from our

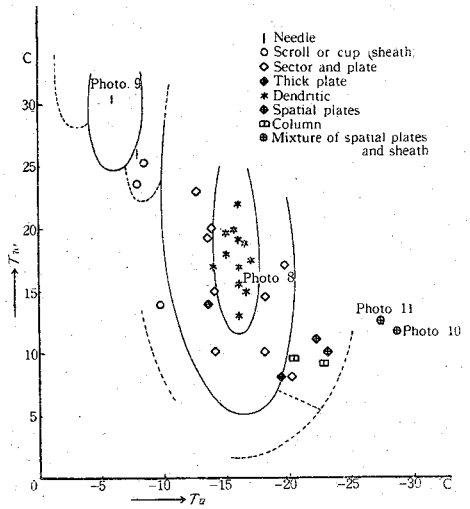

Fig. 4. T_a-T_w diagram; the ordinary air.

old T_a–T_w diagram[4]. The result shows that the former T_a–T_w diagram obtained with the different apparatus can be applied in this series of experiments.

A typical dendritic crystal, which is obtained at $T_a=-16.0$°C and $T_w=+15.5$°C, is shown in Photo. 8, Pl. II. The condition of formation is just in the middle of the dendritic region, Fig. 4. After the dendritic crystal is made, the condition is changed to that of the needle region. Beautiful needles grow perpendicularly from the basal crystal, the side view of which is shown in Photo. 9, Pl. II. The condition for needle formation was $T_a=-6.1$°C and $T_w=+30.5$°C in this case. Two examples of crystals made at lower temperatures are shown in Photos. 10 and 11, Pl. II; $T_a=-28.8$°C and $T_w=+11.8$°C for Photo. 11 and $T_a=-27.5$°C and $T_w=+12.5$°C for Photo. 10. The crystal usually takes the form of spatial assemblage of plates, Photo. 10, and sheath-like crystal is also obtained, Photo. 11. This result also agrees with our former experiment.

d) The condition of formation of snow crystals in aerosol free air.

The similar experiment was carried out by using aerosol free air in the wide range of temperature between −1°C and −36°C. The condition of formation of various types of crystals in aerosol free

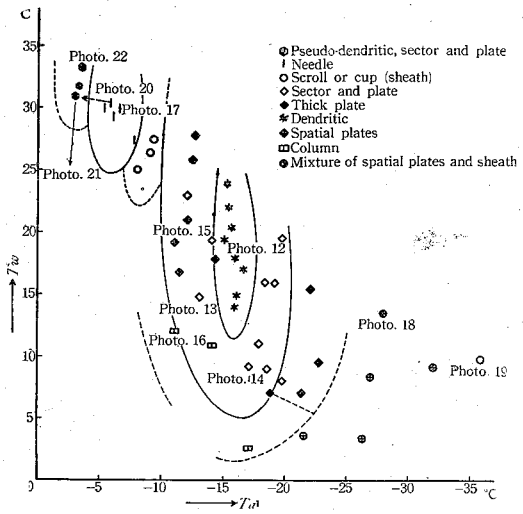

Fig. 5. T_a-T_w diagram; the aerosol free air.

air was found to be almost the same as that in the case of ordinary air. The results are shown in Fig. 5, in which the boundary curves are the same as those in Fig. 4. Generally speaking, it was confirmed that the aerosol particles do not affect the condition of formation of snow crystals and the shape of crystal is determined by two elements; that is, the temperature and the water excess in the atmosphere. Examples of the dendritic, broad branches, sector, thick plate, column and needle, which are obtained in the aerosol free air, are illustrated in Photos. 12–17, Pl. III. The condition of formation of each of them is seen Fig. 5. The condition of the crystal Photo. 13 is that of the later stage of crystal growth, in which the crystal developed in the shape of plate. The crystal of Photo. 18, Pl. IV, is made at $T_a = -27.9$°C and $T_w = +13.5$°C, which condition is similar to that of Photo. 11, Pl. II. The crystal is the mixture of spatial plates and sheath-like crystals, and the shape is very similar to that of Photo. 11. No essential difference is noticed between the ordinary air and the aerosol free air in this colder region. Photo. 19, Pl. IV, shows the crystals made in aerosol free air at $T_a = -35.8$°C and $T_w = +9.8$°C. This is the coldest temperature tested in this series of experiments. The crystal developed in a typical sheath shape. It must be mentioned that

the tendency of crystal to develop in the direction of principal axis is observed in two temperature regions; the one is the warmer region where the needles and cups are obtained and the other is the colder region around −30°C where the sheath is observed.

The marked difference between the ordinary air and the aerosol free air was observed in the warmer region near the freezing point. When the ordinary air is used, the temperature range between −1°C and −4°C is the region of irregular assemblage of needles Many photographs of the crystals of this type are reproduced in "Snow Crystals", and a typical one is illustrated in Photo. 23, Pl. IV. Many curved needles become a bundle in this case, as seen in the photograph. It is confirmed that, when the aerosol free air is used, the crystal shows the tendency to develop in the basal plane in this region. The crystal shown in Photo. 20, Pl. IV, was made in the needle region, $T_a = -5.8$°C and $T_w = +30.3$°C, and the crystal developed as thick needles. Then the condition was changed to the region corresponding to the irregular needles in the case of the ordinary air; $T_a = -3.0$°C and $T_w = +31.0$°C. The tip of the needle starts to grow in the basal plane. Photo. 20 shows the side view of this stage. Waiting a little while, the basal plane develops into a hexagonal plate, the front view of which is reproduced in Photo. 21, Pl. IV. It is a new fact that plate type is obtained near 0°C in the case of aerosol free air. This plate type develops into an apparently dendritic form when the crystal is kept in this condition for a while. This type is different in internal structure from the ordinary dendritic crystal. The structure is such that many small plates are assembled in the dendritic form. One examples is shown in Photo. 22, Pl. IV. This is called the "pseudo-dendritic" type.

The effect of aerosol particles in the air is summerized as follows. No essential difference is observed in the whole range tested, except the warmer region between −1°C and −4°C. This region is "irregular needle" for the ordinary air, but it becomes "pseudo-dendritic" for the aerosol free air.

§3. Mechanism of attachment of droplets to ice surface.

a) Water droplets in the snow making apparatus.

When the ordinary air is used, many fog particles appear in

the snow making apparatus and they give the Tyndall scattering of light, as shown in Photo. 1, Pl. I. The size distribution of these fog particles was studied under the condition of snow formation. From the spot near the growing snow crystal, a certain amount of air is sucked and it is impacted to an oil film so that fog pasticles are captured in the oil film. The technique is the same as the ordinary method of fog counting.

Two examples are shown in Fig. 6. The white circles show the size distribution when $T_a = -12°C$ and $T_w = +17.5°C$; that is the

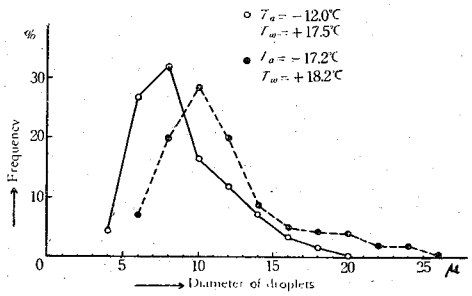

Fig. 6. Size distribution of fog particles in the snow making apparatus.

condition of sector formation. The dark circles are the condition of dendritic formation, $T_a = -17.2°C$ and $T_w = +18.2°C$.

The maximum frequency is observed at the diameter of 8μ in the former case, and it is at 10μ in the latter case when the supersaturation is larger. The crystals usually grow in an unrimed state under these conditions. Sometimes rimed crystals are obtained, but most of the droplets frozen to the surface of snow crystal are large, the diameter being larger than 15μ. The smaller droplets do not freeze to ice surface in the droplet form. There are two explanations for this phenomenon. The one is the sudden evaporation of droplet at the very vicinity of ice surface. If the droplet is pure water and GIBBS-THOMSON formula of the effect of surface tension is applicable, the minute droplet must evaporate in a very short time of the order of a few hundredths of a second at the very vicinity of ice surface. This calculation is made by AUFM KAMPE[5] and others. If this is the case, the growth of snow crystal is a phenomenon taking place in vapor phase. This is the

ordinary conception of sublimation; that is, the direct condensation from vapor to ice surface will be the main process of snow formation, but there may be another process besides this sublimation phenomenon. The minute droplets may hit the ice surface before complete evaporation, and they spread over the ice surface before freezing. In this case no riming is observed and the result is the same as the sublimation. The spreading of a supercooled droplet on the ice surface can be expected, if we assume a liquid-like film on the surface of ice at the temperature below freezing. The presence of such a film on the ice surface was inferred by WEYL[6] from theoretical point of view, and the experimental evidences was shown by NAKAYA and MATSUMOTO[7], and HOSLER and others[8] also confirmed the result obtained by NAKAYA and MATSUMOTO.

From these considerations, the mechanism of attachment of supercooled water droplets to ice surface is an interesting problem. We, therefore, proceeded to study this problem by the method of microcinematography under high magnification.

b) The apparatus for microcinematography.

The mechanism of attachment of minute droplets to ice surface was studied by the method of microcinematography. The apparatus is shown in Fig. 7. The whole system is set in the cold room at about −30°C. The warm water vapor evaporated from the heated reservoir goes up by natural convection and passes through the rectangular canal made of brass. The temperature t in this canal is measured, and it is regulated so that t is about −10°C. The excessive moisture condenses in this canal as steam fog, and the air stream containing these supercooled droplets is conveyed into the experimentation box made of transparent plastics. A thin ice sample frozen to a mesh or a deck glass is set in a slightly slanted position, as shown in Fig. 7. Minute droplets suspended in the air stream hit the surface of ice sample and attach to the surface. The mode of attachment is studied by transmitted light with the 16 mm cine-camera through a microscope under the magnification of about 200. The temperature of air T_a near the ice surface is measured, and it is regulated in the range between −13°C and −20°C. The minute droplets in the air stream are considered to be supercooled to at least −10°C. About 600 ft of film was run

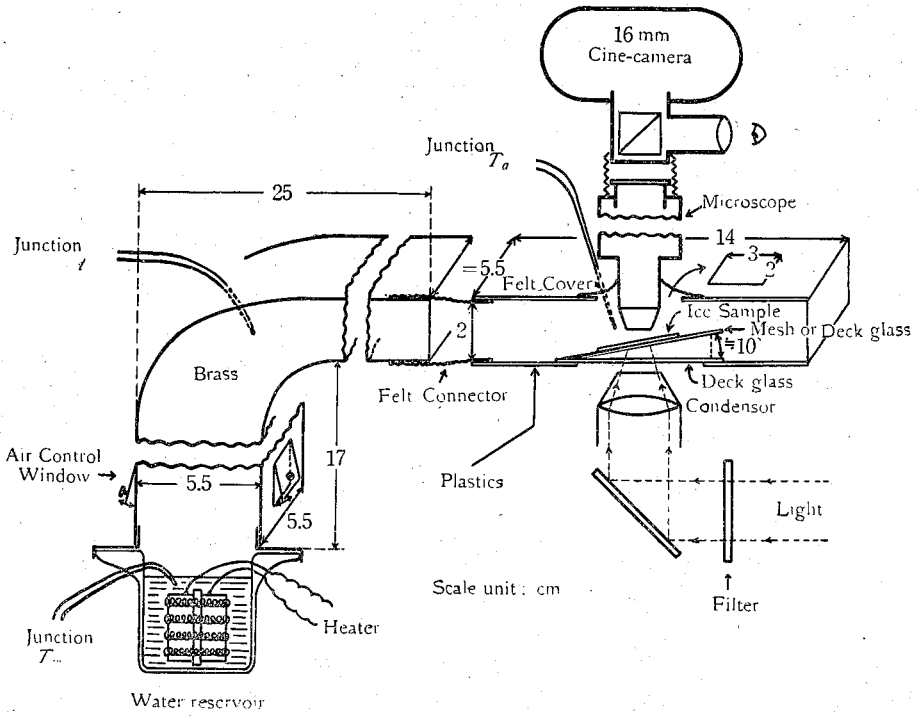

Fig. 7. Apparatus for microcinematography.

and the mechanism of attachment of these supercooled droplets to ice surface was studied with respect to various states of the ice surface.

c) The mode of attachment of minute droplets on the old or contaminated ice surface.

The ordinary commercial ice is cut in a plate of the required shape and is frozen to a deck glass. When this sample is kept in the cold room for a few days, the surface is etched by natural sublimation and shows an appearance like the surface of pigskin under the microscope. When the air stream containing supercooled droplets is sent to this surface, a very interesting phenomenon is observed. The droplet does neither freeze in the droplet form nor evaporate immediately, but it rolls over the ice surface for some distance. The droplet usually becomes smaller and smaller while rolling over the ice surface, and vanishes in the short time

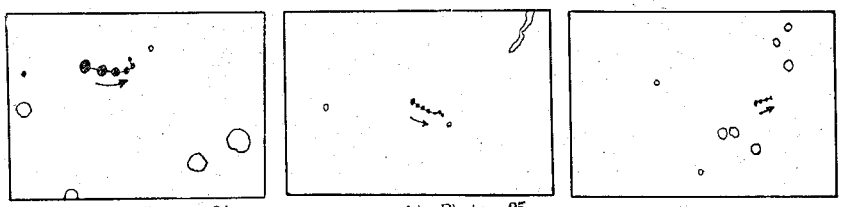

a) Photo. 24 b) Photo. 25 c) Photo. 26

Fig. 8 a)-c). Rolling of droplet on the ice surface.

of the order of half a second or so. One example is shown in Photo. 24, Pl. V, the condition being $T_a=-15°C$, $T_w=+30.0°C$ and $t=-9.5°C$. A droplet of about 5μ in diameter hits the surface in b), and this droplet rolls over the ice surface as shown in c)-f), and vanishes just after f). The time required for the complete evaporation is 0.5 sec and it travelled on the surface for the distance of about 27μ. The track is shown in Fig. 8 a), which is copied from Photo. 24 b)-f). Photo. 25, Pl. V, shows the mode of rolling of a droplet when the polished surface of ice is melted by radiation from a spot light and then refrozen. The behavior of the droplet is almost the same as before. The condition is $T_a=-13.5°C$, $T_w=+24.0°C$ and $t=-9°C$. A droplet hits the ice surface in a) and then rolls over the surface as shown in b)-f). The track is shown in Fig. 8 b). The initial size of the droplet is about 4.5μ, and this becomes smaller and smaller while rolling, and evaporates completely in 0.4 sec after travelling about 30μ. It looks as if the contamination is not removed.

The behavior of the droplet is like that of rain drop rolling over the water surface of a pond, which phenomenon is often observed in the case of heavy rain. This phenomenon is known to be due to the gas molecules adsorbed on the surface of rain drop. In the present case, the most probable reason is considered to be the effect of contamination of ice surface. In order to check this point, the surface of ice was rubbed slightly with a cotton cloth containing a trace of oil. The rolling of droplet was remarkable in this case, and the travelling distance sometimes was much larger than the field of microscope.

d) The mode of attachment of droplet on the new clean ice surface.

In order to study the mode of attachment when the ice sur-

face is clean, three kinds of ice surface were prepared. The one is the new surface of ice obtained by breaking an ice block. When this surface is used, the rolling of a droplet is not conspicuous, but it is observed that the droplet slides on the surface for a short distance and the track of sliding of the droplet is visible on the ice surface for a short time after the droplet is completely disappeared. One example is shown in Photo. 26, Pl. VI and Fig. 8 c), the coadition being $T_a=-19.0°C$, $T_w=+22.0°C$ and $t\fallingdotseq-11°C$. A minute droplet about 3μ in diameter hits the ice surface in b). It slides on the ice surface towards the right-side in the picture, as shown in c)–f), and disappears. The sliding distance is about 16μ and the time required is 0.25 sec. It is interesting to notice that the track of sliding of the droplet on the ice surface remains visible after the droplet disappeared, Photo. 26 g). In this case the track appears bright, but it becomes a dark line when the mode of illumination is changed slightly. It is understood from this fact that this track is a tiny ridge left on the ice surface. This ridge disappears in several minutes.

The second kind of clean ice surface is obtained by washing the ice surface with distilled water. The skin of the ice sample is melted off by this method, and new surface of ice appears. The tracks caused by sliding of droplets on the ice surface are also visible in this case. Successive stages of appearance of tracks are photographed with one minute interval and are shown in Photo. 27, Pl. VI. In this case the ice sample was set near the outlet of the canal so that many droplets can hit the surface. The condition is such that $T_a=-17°C$, $T_w=+40°C$, $t=-7°C$. One minute after exposed to the air stream, the first track appears, as shown in b). The number of tracks increases fairly rapidly and more than ten tracks are visible in e), $t=4$ min.

The third kind of clean ice surface is obtained by making discoid crystal of ice. When slightly supercooled water is seeded with tiny ice fog particles, crystals of ice in the shape of thin discoid are obtained. The flat surface of this discoid is the basal plane of the hexagonal system of ice crystal. When the surface of this discoid crystal is used, exactly the same phenomenon is observed as described above.

Throughout this series of experiments, it was found that the

rolling of droplet or the sliding on the ice surface is observed when the droplets is small, being less them 5μ in diameter. In the case of rimed snow crystals observable in nature, it is known that the diameter of fog particles frozen to snow crystals is larger than 5μ. It is very probable that the same phenomenon as the present result takes place in the case of natural snow crystals, and the smaller droplets less than 5μ in diameter spread over the surface of snow crystal when they hit the surface.

§ 4. The nature of ice surface and sublimation process.

a) The migration of powder on snow crystal due to sublimation.

It has been noticed by many people that dust particles scattered on the surface of snow crystal migrate on the surface as the crystal evaporates by sublimation. YOSIDA and collegues[9] studied the mode of migration of dust particles and observed that the track of the particle is perpendicular to the evaporating edge of the snow crystal. This is an interesting phenomenon for the study of the mechanism of sublimation process. If sublimation takes place by the direct evaporation of water molecule from the crystal lattice of ice, the dust particle must remain at the original spot. There can be no dragging force to cause the migration of the dust particle. The simplest way of explaining the origin of this dragging force is to assume the presence of liquid-like film on the ice surface. From this consideration, the mode of migration of dust particles caused by the sublimation of snow crystal was studies in detail.

b) The experiments.

The mode of sublimation of snow crystals was investigated for 58 samples, extending over the temperature range between $-5°C$ and $-40°C$. In the earlier stage the snow crystal was kept on a glass plate, but in the later experiments it was put on a nylon mesh. The filament was 15μ in diameter, and the size of mesh was 0.05 mm. The experiment was carried out in a thermostat box with the constancy of $\pm 0.5°C$. The snow crystal is kept in darkness, and the illumination is given at the moment of photography only. The fine powder of carbon black is used as the dust particle. The carbon black is fully desiccated before using.

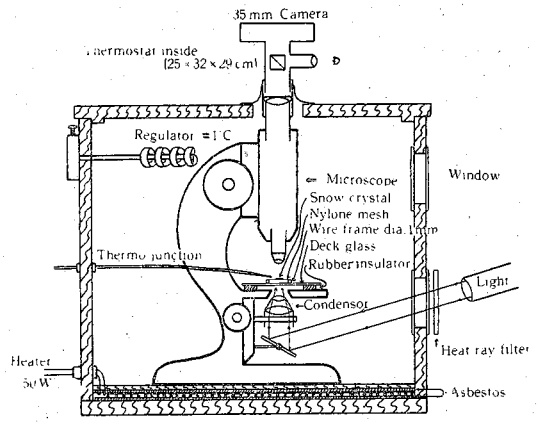

Fig. 9. Apparatus for the study of sublimation process.

One example of the mode of sublimation of a dendritic crystal is shown in Photos. 28–33, Pl. VII. The crystal is kept on a nylon mesh, and the temperature is kept at −25°C. The crystal evaporated within one hour at this temperature. The carbon powders are drawn towards the center as sublimation proceeds. It is noticed that most of the carbon powders stick to the edge of snow crystal and are suspended in air. The successive stages of sublimation of the crystal and the trajectories of the powders are copied and shown in Fig. 10. The trajectory is always perpendicular to the evaporating edge of the crystal. The velocity of migration v; that is, the linear velocity of sublimation, was measured for 4 particles and the mean was about 0.01 mm/m.

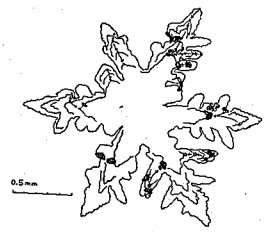

Fig. 10. Sublimation of dendritic crystal. Sample No. 57, $\theta = -25°C$, $v = 0.01$ mm/m.

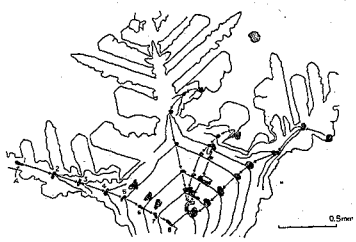

Fig. 11. Sublimation of plate with dendritic extensions. Sample No. 11. $\theta = -4°C$, $v = 0.1$ mm/m.

A crystal of plate form with dendritic extensions was studied in the same way; Photos. 34–39, Pl. VIII. The sample was put on a glass plate, and the temperature was kept at −4°C. At this higher temperature, the crystal almost evaporated within 15 m. The particle A in Photo. 34 is rotated in Photo. 35, as one point of the powder is dragged by the evaporating crystal. The main part A of this powder looks to have stuck to glass surface, and the portion A′ is dragged by the crystal. This dragging force is strong enough to break this powder, and the portion A′ moves with the crystal, while the portion A remains on the glass plate; Photo. 36. Such dragging force cannot be explained, if the sublimation is a process of direct liberation of each water molecule from ice lattice. In Photo. 37, the fragment A′ of the powder A is very near to another particle B, but these two particles A′ and B are separated afterwards; Photo. 38. The mode of migration of these particles are well illusrated in Fig. 11. The mean of migration velocities of 4 particles is 0.1 mm/m.

The migration of powder due to sublimation of snow crystal takes place at very low temperatures below −30°C. Photos. 40–43, Pl. IX, show the mode of sublimation of a fern-like crystal at the temperature which varied between −28°C and −40°C. At such low temperatures, the sublimation process is very slow and it took more than 30 h for the complete evaporation. The migration of the powder takes place also at this low temperature. Two other examples of dendritic crystals are shown in Figs. 12 and 13. The mode of migration of particles is more or less the same, and the sublimation velocity at −7°C is 0.2 mm/m, and that at −20°C is 0.02 mm/m.

The linear sublimation velocity is not only the function of temperature, but it varies considerably for different types of crystals. At the same temperature, the sublimation velocity is smaller for the crystal of broad branches than the case of dendritic one. Fig. 14 is an example of broad branches, and the mean velocity of sublimation is one half of the dendritic crystal, Fig. 13. Fig. 15 is a sector type, and the velocity is only 0.003 mm/m at −18.8°C. The surface area per unit mass is smaller in the order of dendritic, broad branches, sector. The linear sublimation velocity must be in the reverse order, and the result of experiments agrees

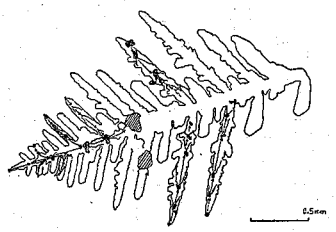

Fig. 12. Dendritic crystal; Sample No. 13, $\theta = -7°C$, $v = 0.2$ mm/m.

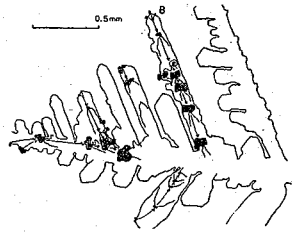

Fig. 13. Dendritic crystal; Sample No. 23, $\theta = -20°C$, $v = 0.02$ mm/m.

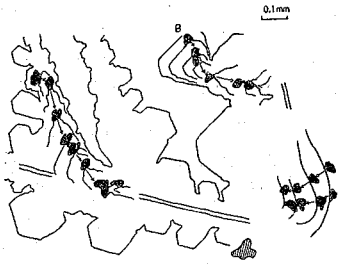

Fig. 14. Broad branches; Sample No. 21, $\theta = -18°C$, $v = 0.01$ mm/m.

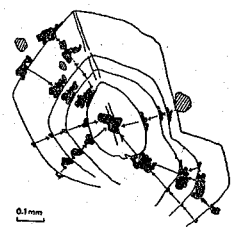

Fig. 15. Sector; Sample No. 22, $\theta = -18.8°C$, $v = 0.003$ mm/m.

with this expectation.

c) Relation between the linear sublimation velocity and temperature.

The linear sublimation velocity of snow crystals decreases very rapidly with decrease in temperature. With respects to 5 samples, which show a regular mode of displacement, the amount of displacement of a particle is measured as the function of time. The result is shown in Fig. 16. The linear sublimation velocity becomes very small when the temperature goes lower, and the dendritic crystal evaporates faster than the broad branch type or the plate. In these cases the linear sublimation velocity can be taken as constant, but this is not always the case. Taking the mean of several particles scattered on the surface of a crystal, the logarithm of velocity is plotted against temperature in Fig. 17. As the first approximation, the linear relation is observed for the upper and lower limits respectively, and the points lie within

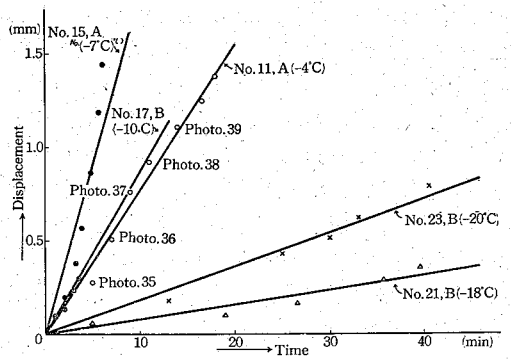

Fig. 16. Displacement of particle versus time.

this band. The width of this band is due to the difference in crystal type, and the points for sector and broad branches are seen always below those of dendritic type at the same temperature.

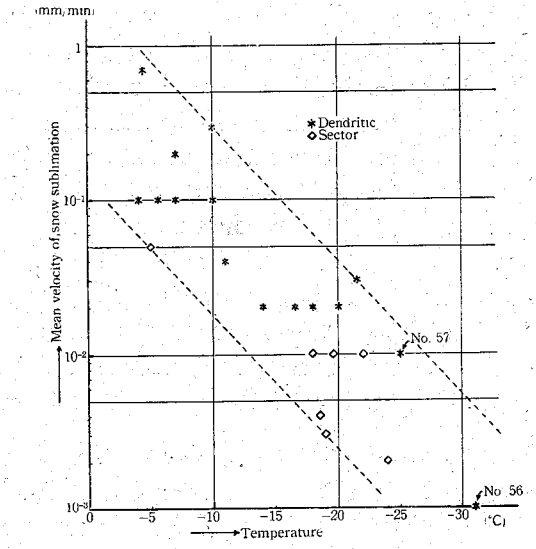

Fig. 17. Relation between sublimation velocity and temperature.

d) Sublimation of other volatile solids.

The similar experiment was repeated by using the blocks of camphor, naphthalen and para-dichlor-benzol. The sample is cut in the form of a plate, and carbon powder was scattered on the sur-

face. This sample is kept at the room temperature, and the migration of the powder due to evaporation of the sample is observed under a microscope. The same phenomenon is seen as the case of snow crystal. The powder sticks to the edge of the sample and is dragged towards inside, as the sample evaporates. Two photographs showing this process in the case of para-dichlor-benzol are reproduced in Photos. 44 and 45, Pl. IX.

The results of the experiment described above are considered to show another evidence of existence of liquid-like film on the surface of ice, and the sublimation of ice is a process of evaporation of this liquid-like film into vapor phase. The similar mechanism is inferred to exist in the process of sublimation of other volatile solids.

§ 5. Effect of impurity in air on the shape of snow crystals.

In the earlier experiments on the effect of aerosol particles, the same arrangement as shown in Fig 3 was used, but the liquid air trap and the bubbling flow-meter were not attached. A flow-meter containing silicone oil of 5 c. s. was used instead of the bubbling flow-meter. The thermal impactor worked in a good condition, and no fog was observed in the cloud chamber. Snow crystals formed in this aerosol free air took the needle shape in the wide range of temperature, corresponding to the dendritic and plate regions. At first this result was misunderstood to show the effect of aerosol free air, but later experiments revealed that this effect was due to the trace of silicone vapor evaporated from the flow-meter. The effect of impurity, therefore, was studied in detail as the controlling factor of the snow crystal shape.

a) Effect of silicone vapor on the shape of snow crystals.

The silicone oil used in the flow-meter in the earlier stage was KF96L produced by Shinetsu Chemical Co. The viscosity is 5 c.s., but this is a blended material and contains volatile constituent. In order to study the effect of silicone oil vapor, 4 kinds of D. C. 200 F were tested; 0.65 c.s., 3 c.s., 10 c.s. and 30,000 c.s. The specimens of 10 c.s. and 30,000 c.s. showed no effect. The specimen of 3 c.s. showed a considerable effect, transforming the dendritic type into a sheath-like crystal. The most remarkable effect was

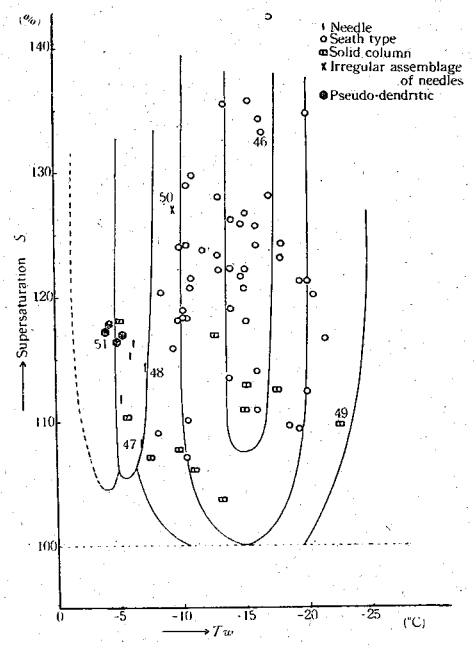

Fig. 18. Temperature-supersaturation (T_a–s) diagram; aerosol free air with silicone vapor.

observed when the specimen of 0.65 c.s. was used.

Fig. 18 shows the temperature-supersaturation (T_a–s) diagram for the aerosol free air with trace of silicone vapor. The supersaturation s was measured by passing a known quantity of air through the P_2O_5 plug, and the amount of water was measured by a chemical balance. The details of this technique are described in "Snow Crystals"[10]. It is remarkable that such a high supersaturation as 140% is obtained in purely gaseous state of water vapor. No fog particle was observed in this high supersaturation. In the dendritic, plate and cup regions of the ordinary air, the crystal developed into elongated sheath-like shape. One example of this sheath-like crystal obtained in the dendritic region is shown in Phot. 46, Pl. X; $T_a=-16.5°C$, $T_w=+16.5°C$, $s=133.3\%$. It is interesting to notice that this crystal is very similar to that shown in Photo. 19, Pl. IV, which was obtained at $T_a=-35.8°C$ in the aerosol free pure air. The effect of silicone oil vapor corresponds to the decrease in temperature. In the needle region of the

ordinary air, the crystal is still needle; Photo. 47, Pl. X ($T_a=-6.5°C$, $T_w=+27.6°C$, $s=107\%$) and Photo. 48 ($T_a=-7.2°C$, $T_w=+16.2°C$ $s=114.3\%$). Usually the needle is very slender in this case, Photo. 47, and sometimes the surface of needle is smooth, Photo. 48. Photo. 49, Pl. X, is a column which is obtained in the spatial plates region, as shown in Fig. 18 ($T_a=-22.5°C$, $T_w=+10°C$, $s=109.9\%$). In the cup region of the pure air, an assemblage of needles is sometimes observed besides the elongated sheath-like crystals. One example is shown in Photo. 50, Pl. X ($T_a=-9.5°C$, $T_w=+26.8°C$, $s=127.1\%$). The effect of aerosol free air was observed in the irregular needle region, as already described in §2 d); the pseudo-dendritic crystals having been obtained in this region when aerosol particles were removed; Photo. 22, Pl. IV. When silicone vapor is added to the aerosol free air, no effect is observed in this region; that is, the pseudo-dendritic type is also obtained. One example is shown in Photo. 51, Pl. X ($T_a=-4.0°C$, $T_w=+26.8°C$, $s=117.3\%$), which is to be compared wifh Photo. 22, Pl. IV. The effect of removing aerosol particles and that of silicone vapor are tabulated in Table. I.

TABLE I. Effect of removing aerosol particles and adding silicone vapor.

Ordinary air	Aerosol free air	Aerosol free air+silicone vapor
irregular needle	pseudo-dendritic*	pseudo-dendritic*
needle	needle	needle
cup	cup	sheath, bundle of needles*
plate and sector	plate and sector	sheath*
dendritic	dendritic	sheath*
column	column	column
spatial plates	spatial plates	column*

*Effect is evident.

b) Effect of acetone vapor on the shape of snow crystals.

Effect of impurities on the shape of snow crystals was examined by SCHAEFER[11] by using various chemicals. Among them acetone vapor was one of the most effective material. This experiment was repeated and the effect was studied as the function of the

acetone vapor. In order to change the percentage, a trap containing cotton ball soaked with liquid acetone was used. The aerosol free air was sent to the snow making apparatus after passing this trap. The percentage of vapor was varied by changing the temperature of this trap. The rate of air flow in the trap was kept at 3.5 c.c./sec. The air is assumed to be saturated with acetone vapor at the trap temperature T, and this air is warmed up to the temperature of the dendritic region at about $-15°C$. Let the saturation vapor pressure of aceton at T be p. The volume V of one mole of acetone vapor at T is

$$V = \frac{p_0}{p}\frac{T}{T_0} V_0 ,$$

where p_0 and T_0 show the standard condition, and $V_0 = 22.4 \times 10^3$ c.c. Let the number of acetone molecules per c.c. at T be N_T.

$$N_T = \frac{N_0}{V} ,$$

Where N_0 is AVOGADRO's constant 6.02×10^{23}. The number of molecules N_{-15} in the dendritic condition at $-15°C$ is

$$N_{-15} = \frac{T}{T_{-15}} N_T ,$$

$$\therefore \qquad N_{-15} = \frac{pT_0N_0}{p_0T_{-15}V_0} . \qquad (1)$$

The number of water molecules per c.c. at $-15°C$ in the condition of supersaturation of 130% is

$$N'_{-15} = 6.0 \times 10^{16} . \qquad (2)$$

The vapor pressure of acetone at low temperatures was cited from the International Critical Table, and the values at required temperatures are obtained by interpolation. The percentage of acetone vapor in air and the ratio of numbers of water and acetone molecules in the condition of crystal growth are given in Table II.

The results of experiments are shown in Photos. 52–57, Pl. XI. As the blank test, the aerosol free air is passed through the liquid air trap without containing acetone, and the crystal is made at $T_a = -15.9°C$ and $T_w = +18.3°C$. The crystal develops into a dendritic

TABLE II. Number of acetone molecules.

Photo. No.	T	p, mmHg	N_{-15}/c.c.	Percentage in air	H_2O : Acetone
53	−180°C	0.00001*	3.74×10^{11}	1.3×10^{-8}	1 : 0.000006
55	− 74°C	0.18	0.67×10^{16}	2.4×10^{-4}	1 : 0.11
56	− 56°C	1.3	4.85×10^{16}	1.7×10^{-3}	1 : 0.83
56	− 49°C	2.4	9.0×10^{16}	3.2×10^{-3}	1 : 1.5
57	− 22°C	13.4	4.9×10^{17}	1.76×10^{-2}	1 : 8.2

* extrapolated; rough estimate.

type, as shown in Phot. 52, Pl. XI. Photo. 53, Pl. XI, shows the crystal made at $T_a=-16.0$°C and $T_w=+17.5$°C, when the acetone ball is put in the trap kept at liquid air temperature −180°C. It is an interesting fact that such a small quantity of acetone vapor as 1.3×10^{-8} as impurity gives the effect; that is, transforming the dendritic type into the broad branch type. The crystal of Photo. 54, Pl. XI, is made while T is increased from −180°C to −74°C. The percentage of acetone vapor is increased from 1.3×10^{-8} to 2.4×10^{-4} during the course of crystal growth, the condition of formation being $T_a=-15.5$°C and $T_w=+18.0$°C. The crystal of a shallow dish shape is obtained. When the crystal is made with acetone vapor of 2.4×10^{-4} in air from the beginning, the crystal grows into a hexagonal column with skeleton structure; Photo. 55, Pl. XI, which is made at $T_a=-15.0$°C and $T_w=+20.0$°C. The tendency of growing into the direction of principal axis is enhanced. In this case the number of aceton molecules is about one tenth of that of water molecules. Increasing the acetone vapor to the same order of concentration of the water vapor, the tendency of growing in the direction of principal axis is more enhanced, and the crystals of an elongated sheath shape are obtained; Photo. 56, Pl. XI, which is made at $T_a=-16.0$°C and $T_w=+19.5$°C. This is the typical shape hitherto observed as the effect of acetone vapor. When the temperature of the trap is increased to −22°C, the concentration of acetone vapor becomes about ten times of that of water vapor. In this case very thin needle is obtained, as shown in Photo. 57, Pl. XI, the condition is $T_a=-14.5$°C and $T_w=+19.9$°C. The transformation of dendritic type into needle or sheath type

proceeds in a regular way, as the concentration of acetone vapor is increased. According to SCHAEFER's result, acetone in concentrations as low as one molecule of acetone to 100 molecules of water causes the crystal to become either hexagonal column or a peculiar combination of plate and column. The result of the present experiment is concordent with his result.

Some experiments were carried out to check the amount of acetone adsorbed or absorbed in the needle crystals which were produced in the air containing acetone vapor. Many needle crystals of hoar were made in the air with acetone vapor, and they were collected and melted. The acetone concentration of this thaw water was measured by the use of BECKMANN's absorption spectrograph. The calibration curve of this absorption spectrograph is shown in Fig. 19.

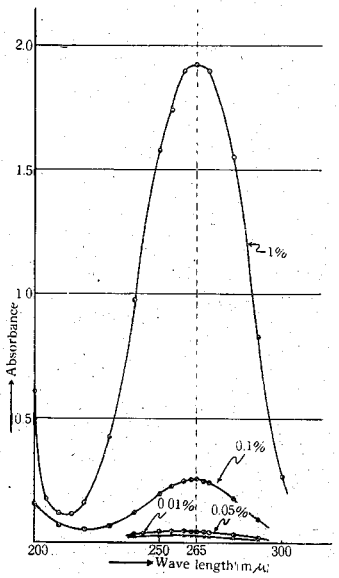

Fig. 19. Calibration curve of BECHMANN's absorption spectrograph.

The absorption of acetone occurs at 265 mμ, and the lower limit of the measurable concentration is between 0.01% and 0.05%. Two examples of the absorption curve of acetone hoar are shown in Fig. 20. A slight maximum is observed in each of the curves, being superposed on the background.

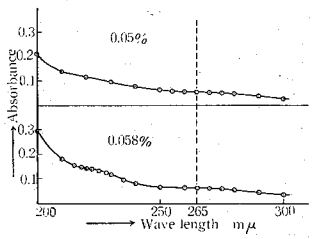

Fig. 20. Absorption curve of the thaw water of acetone hoars.

The estimated percentage of acetone is about 0.05%. It is probable that acetone molecules are adsorbed on the surface of needle crystal and partly occluded in the skeleton structure of the crystal. In order to carry out the parallel experiment, 0.5% solution of acetone was made to freeze in the cold room. When freezing proceeded partly, the ice was picked up and the acetone content of the residual solution was

measured in the same way. The residual solution was found to be concentrated to 0.64%, as shown in Fig. 21. The ice was melted, and the thaw water was tested. This ice contained 0.12% of acetone. A part of this acetone must be due to the liquid film of the residual solution covering the surface of crystal. The similar experiment was repeated, but the ice sample was washed thoroughly with pure water at 0°C before being melted. The thaw water of this washed ice showed the acetone content of 0.05%, the same value as the hoar crystals produced in the air with acetone vapor. The most part of this 0.05% acetone is considered to be the acetone molecules adsorbed on the surface of ice crystal.

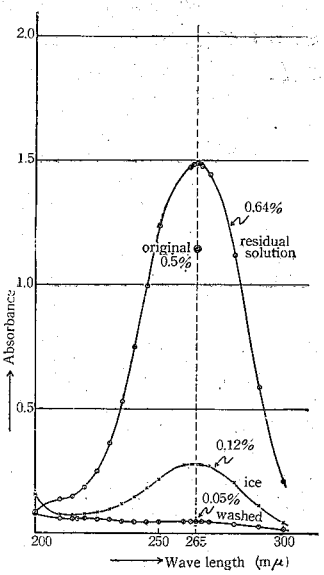

Fig. 21. Acetone content of the ice formed in the dilute solution of acetone.

c) Effect of various vapors on the shape of snow crystals.

In order to look for the effect of vapors on the shape of snow crystals, a cotton ball soaked with the chemicals to be tested was introduced in the upper portion of the snow making apparatus, as shown in Photo. 58, Pl. XII. Acetone was used in this case. The crystals grown on the rabbit hair take the shape of thin needles, which must be due to the effect of acetone vapor evaporated from the cotton ball. Twenty-two kinds of chemicals were tested in the similar way. The results are shown in Table III, and the microphotographs are reproduced in Photos. 58–75, Pls. XII–XIV. All these crystals were made in the dendritic region, T_a having been in the range between -15°C and -17.5°C and T_w between $+16.2$°C and $+20.5$°C.

In Table III, two organic chemicals classified as A give the most marked effect. The crystals develop into thin needles, as shown in Photos. 58 and 59, Pl. XII. Three organic chemicals classified as B are a little less effective, and crystals of slender sheath type are obtained. The microphotographs are shown in Photos. 60–

62, Pl. XII. The other three organic vapors classified as C give typical sheath type; Photo. 63, Pl. XII, and Photos. 64 aud 65, Pl. XIII. The effect of benzol is remarkable and crystals develop into a beautiful scroll type, as shown in Photo. 65, Pl. XIII. The completely developed crystal assumes the form of a scroll folded hexagonally.

The crystals of Photos. 66–69, Pl. XIII, show a peculiar shape. They are classified as C′ in Table III. As a whole the crystal grows into a sheath or cup shape, but prism planes appear at the corners of the hexagonal cup. The structure is well demonstrated in the case of toluene vapor; Photo. 66, Pl. XIII. It is interesting to notice that such a peculiar effect is observed in the case of toluene which is insoluble in water. Similar effect is observed in the case of ether and chroloform. One good example of this prism plane is seen in the case of formalin, Photo. 69. Dichloroethane also gives the similar effect. These five chemicals are grouped as C′ in Table III.

Four chemicals classified as D in Table III; that is, methyl and ethyl alcohols and others, transform the dendritic shape into irregular sector or pseudo-dendritic form. The tendency of developing in the dircetion of principal axis is slight in this case. One example of the irregular sector, which is obtained as the effect of methyl alcohol, is shown in Photo. 71, Pl. XIV. When the vapor of ethyl alcohol is added, the crystal grows into the form of a hexagonal dish, as shown in Photo. 72, Pl. XIV. The side view of the same crystal is shown in Photo. 73. On the back-side of the dish, many minute crystals are observed along the ridges of the hexagonal dish, being orientated in the same way as the main crystal. Carbon tetrachloride, Photo. 74, gives the smilar effect as for the inner structure as methyl alcohol, Photo. 71, but the crystal shows the tendency to develop into a pseudo-dendritic form. When the vapor of nitric acid or hydrochloric acid is added, the crystal grows in an irregular pseudo-dendritic form, as shown in Photo. 75, Pl. XIV. It looks as if the condensation of these vapors on the surface of the growing crystal generates heat and the surface of the snow crystal is partly melted. Two vapors among twenty-two kinds tested; that is, carbon disulfide and ammonia, were found to give no effect on the shape of snow crystals.

TABLE III. Effect of various vapors on

Classification of snow crystals		The chemicals	Photo. No.	Chemical formula	
		Water		H_2O	H_2O
Organic vapors	A	Acetone (propanone)	58	CH_3COCH_3	C_3H_6O
		Methyle ethyl ketone (butanone)	59	$CH_3 \cdot CO \cdot C_2H_5$	C_4H_8O
	B	Diethylene oxide (1.4-dioxane)	60	$O \cdot C_2H_4 \cdot O \cdot C_2H_4$	$C_4H_8O_2$
		Amyl-acetate (iso)	61	$CH_3CO_2C_2H_4CH(CH_3)_2$	$C_7H_{14}O_2$
		Acetic acid glacial (99%)	62	CH_3COOH	$C_2H_4O_2$
	C	Butyl alcohol (n) (butanol-1)	63	$C_2H_5CH_2CH_2OH$	$C_4H_{10}O$
		Methylene chloride (dichloro methane)	64	CH_2Cl_2	CH_2Cl_2
		Benzene (Benzol)	65	C_6H_6	C_6H_6
	C′	Toluene (Toluol) (Me-benzene)	66	$CH_3 \cdot C_6H_5$	C_7H_8
		Ether (di-ethyl ether)	67	$(C_2H_5)_2O$	$C_4H_{10}O$
		Chloroform (Trichloro methane)	68	$CHCl_3$	$CHCl_3$
		Formalin (40% Formaldehyde)	69	$H \cdot CHO$	CH_2O
		Dichloro ethane (Ethylene chloride)		$ClCH_2 \cdot CH_2Cl$	$C_2H_4Cl_2$
	B-C-D	Caprylic acid (n) (Octanic acid)	70	$CH_3(CH_2)_6CO_2H$	$C_8H_{16}O_2$
	D	Methyl alcohol (wood alcohol)	71	$CH_3 \cdot OH$	CH_4O
		Ethyl alcohol (ethanol)	72, 73	$CH_3 \cdot CH_2OH$	C_2H_6O
		Trichloro-ethylene (ethylene trichloride)		$Cl \cdot CH ; CCl_2$	C_2HCl_3
		Carbon tetrachloride (tetrachloro methane)	74	CCl_4	CCl_4
	✳	Carbon disulfide		CS_2	
Inorganic vapors	✳	Aqueus ammonia (28%)		NH_3	
	×	Nitric acid (>63.0%)	75	HNO_3	
		Hydrochloric acid (45.2%)		HCl	

Remarks; A. Needle
B. Slender sheath
C. Regular sheath
C′. Irregular sheath
D. Irregular sector, pseudo-dendritic
✳. Dendritic
×. Irregular pseudo-endritic

the shape of snow crystals.

Molecular weight	Specific gravity	Melting point (°C)	Boiling point (°C)	Solvency (in 100g)			Dipole moment (C.G.S., E.S.U.)	Vapor pressure at ≒ −15°C (mmHg)
				Water	Alcohol	Ether		
18.016	1.000	0.0	100.0				$\times 10^{-18}$ 1.84	1.43
58.08	0.792	− 94.6	56.5	∞	∞	∞	2.85	26
72.10	0.805	− 85.9	79.6	37	∞	∞	2.72	11
88.10	1.033	9.5～10.5	101.0	∞	∞	∞		4
130.18	0.876	solution	142.0	0.25	∞	∞		0.4
60.05	1.049	16.7	118.1	∞	∞	∞	1.73	1.2
74.12	0.810	− 79.9	117.0	9	∞	∞	1.63	0.4
84.94	1.336	− 96.7	40.0	2	∞	∞	1.51	54
78.11	0.879	5.5	80.1	0.07	∞	∞	0	7.5
92.13	0.866	− 95	110.6	insoluble	∞	∞	0.37	2.3
74.12	0.708	α − 116.3 β − 123.3	34.6	7.5	∞	∞	1.14	72
119.39	1.489	− 63.5	61.2	0.82	∞	∞	1.05	24
30.03	0.815	≒ − 92	(− 21)					
98.97	1.256	− 35.3	83.7	0.9	∞	∞		8.5
144.21	0.910	16	237.5	0.07	∞	∞		≪ 1
32.04	0.792	− 97.8	64.7	∞	∞	∞	1.69	10
46.07	0.789	− 112	78.4	∞	∞	∞	1.67	4
131.40	1.466	− 73	87.2	0.1	∞	∞		7.6
153.84	1.595	− 22.6	76.8	0.097	∞	∞	0	13
76.13	1.263	− 108.6	46.3	0.2	∞	∞		60
17.03	0.817	− 77.7	− 33.4				1.47	
63.02	1.502							
36.47	1.48	− 15.4					1.03	

In Table III, the chemicals used as impurity are arranged in the order of effectiveness; that is, those in the higher ranks are more effective than the lower ones in accerelating the growth in the direction of principal axis. Comparing this effectiveness with other physical properties, it is found that it is in the order of dipole moment, except benzene. Those with strong polar nature are generally surface-active and the preferential adsorption on the prism and basal plane of the ice crystal will be the cause of the transformation. This also agrees with SCHAEFER's result. The effect of vapor impurities on the shape of ice crystals was studied by ISONO and collegues[12] and they found the similar result as the present experiment with respect to isoamyl acetate.

§ 6. Summary and discussion.

The physical considerations on the supersaturation in the atmosphere under the condition of snow formation are made, and the supersaturation was estimated to be the saturated air with minute droplets. These minute droplets do not give rise to rimed crystals, but they behave just like vapor condensation when they are attached to snow crystals. The effect of removing these minute droplets from the atmosphere on the shape of snow crystals was studied by removing aerosol particles from the atmospheric air. A thermal impactor was used for this purpose, and 140% supersaturation was obtained in purely gaseous state. The preliminary experiment showed that snow crystals developed into needle type in aerosol free air under the condition of dendritic or plate formation. The later experiment, however, showed that this effect was due to the silicone vapor impurity, which came from a flowmeter using silicone oil. When pure aerosol free air was used, no difference was observed between the ordinary air and the aerosol free air, except the warmer region between $-1°C$ and $-4°C$. This region is "irregular needle" for the ordinary air, but it becomes "pseudo-dendritic" for the aerosol free air. This result agrees with the result of the expedition to the Mauna Loa in Hawaii Island, which was undertaken in order to study the shape of snow crystals observable in the region where the aerosol particles are the least. Almost all types of snow crystals were observed.

The minute droplets which hit the ice surface behave like gaseous condensation. There are two explanation for this phenomenon. The one is the sudden evaporation of droplet at the very vicinity of ice surface, which is possible if GIBBS-THOMSON formula of the effect of surface tension is applicable. Another explanation is the spreading of the droplet when it hits the ice surface. This is possible if the ice surface is covered with a liquid-like film at the temperature below freezing. In order to clarify this mechanism, the mode of attachment of these droplets to ice surface was studied by the method of microcinematography under high magnification. The movie showed that the droplet smaller than 5μ in diameter does neither freeze in droplet shape nor evaporate in the very vicinity of ice surface. When the surface is contaminated, the drop rolls round on the ice surface and becomes smaller while wandering, and then vanishes in half a second or so. The wandering distance of a droplet about 5μ in diameter is of the order of 30μ at $-15°C$. When clean ice surface is used, no wandering is observed, but the droplet slides on the ice surface for several microns, and the track of sliding is observed to remain for several minutes. This track is a tiny ridge left on the ice surface, and disappears in several minutes. This is the mechanism of spreading of a droplet on ice surface. Usually drops larger than 5μ in diameter do not show this phenomenon and freeze on the ice surface in a drop shape and gives rise to a rimed snow crystal.

The nature of ice surface and the mechanism of sublimation were studied from the standpoint of evaporation. Fine dust particles scattered on the ice surface are dragged towards the center, as the sublimation proceeds. If sublimation takes place by the direct evaporation of water molecules from the crystal lattice of ice, the dust particles must remain at the original spots. This phenomenon was studied in detail and came to the conclusion that this is another evidence showing the liquid-like nature of the surface of ice.

The effect of vapor impurities in air on the shape of snow crystals was studied with respect to 22 chemicals, most of them being organic vapors. The vapor with strong polar nature showed the marked effect to accerelate the crystal growth in the direction

of principal axis. The preferential adsorption on the prism and basal plane of ice crystal is very sentive in the case of acetone vapor. Acetone in concentration as low as one molecule of acetone to 100,000 molecules of water molecules causes the dendritic crystal into broad branch type. One acetone molecule to 10 water molecules transform the dendritic shape into a hexagonal column with skeleton structure. As the first approximation, the effectiveness of vapor in accerelating the crystal growth in the direction of principal axis is in the order of strength of dipole moment, except benzene.

The experiments were carried out in the cold room laboratory of Transportation Technical Research Institute, Ministry of Transportation, Mitaka, Tokyo. The authors express their hearty sense of gratitude to the authorities of the Institute for letting us use the facilities of this Institute.

References

1) NAKAYA, U., 1955: Snow crystals and aerosols. J. Fac. Sci. Hokkaido University, Ser. II, 4 pp. 341–354.
2) NAKAYA, U., SUGAYA, J. and SHODA, M., 1957: Report of the Mauna Loa expedition in the winter of 1956–57. J. Fac. Sci. Hokkaido University, Ser. II, 5 pp. 1–36.
3) VOLMER, M. and FLOOD, H., 1934: Tröpfenbildung in Dämpfen. Z. Phys. Chem., 170 pp. 273–285.
4) NAKAYA, U., 1954: *Snow Crystals, natural and artificial.* Harvard University Press, p. 244.
5) AUFM KAMPE, H. J., WEICKMANN, H. K. and KEDESDY, H. H. 1952: Remarks on "Electron-microscope study of snow-crystal nuclei". J. Amer. Met. Soc. 9 pp. 374–375.
6) WEYL, W. A., 1951: Surface structure of water and some of its physical and chemical manifestations. J. Colloid Sci., 6 pp. 389–405.
7) NAKAYA, U. and MATSUMOTO, A., 1954: Simple experiment showing the existence of "liquid water" film on the ice surface. J. Colloid Sci., 9 pp. 41–49.
8) HOSLER, C. H., JENSEN, D. C. and GOLDSHLAK, L., 1957: On the aggregation of ice crystals to form snow. J. Amer. Met. Soc., 14 pp. 415–420.
9) YOSIDA, Z. and Collegues, 1955: Physical studies on deposited snow, I. Contributions from the Institute of Low Temperature Science, Hokkaido University, No. 7, pp. 41–42.
10) NAKAYA, U., 1954: *Snow crystals, natural and artificial.* pp. 246–248.
11) SCHAEFER, V. J., 1949: The formation of ice crystals in the laboratory and the atmosphere. Chem. Rev. 44 pp. 311–315.
12) ISONO, K., KOMABASHI, M. and ONO, A., 1957: On the crystal habit of ice-crystals grown in the atmosphere of hydrogen and carbon dioxide. J. Met. Soc. Japan, Ser. II, 35 p. 337.

1

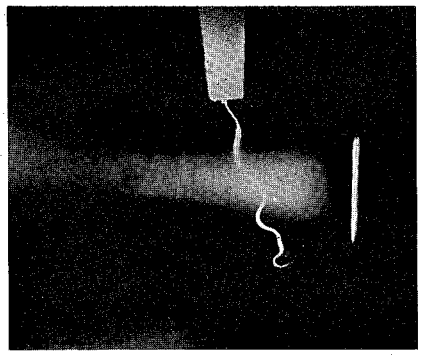

Ordinary air, expos=1 sec. × 1.2

2

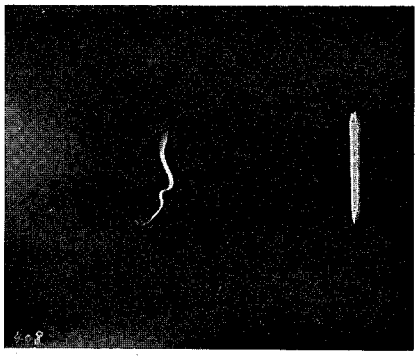

"Aerosol free" air, expos=1 sec. × 1.2

3

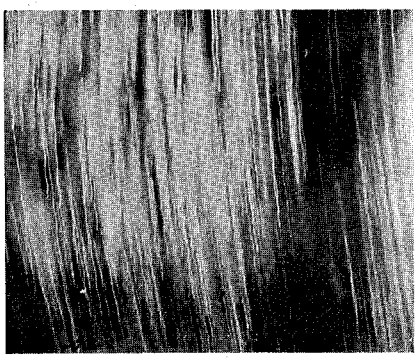

Ordinary air, $s=1.23$, expos=1/4 sec. × 9

4

Filter only, $s=1.23$, expos=1/25 sec. × 9

5

Aerosol free air, $s=1.23$, expos=1/25 sec. × 9

6

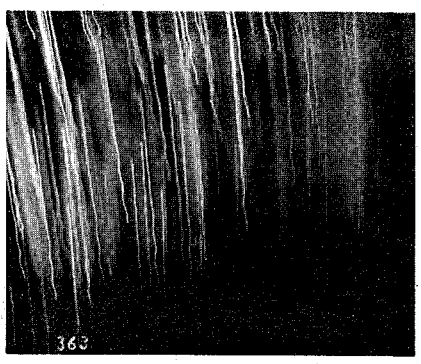

"Aerosol free" air, $s=1.25$, expos=1/4sec. × 9

Ordinary air

7

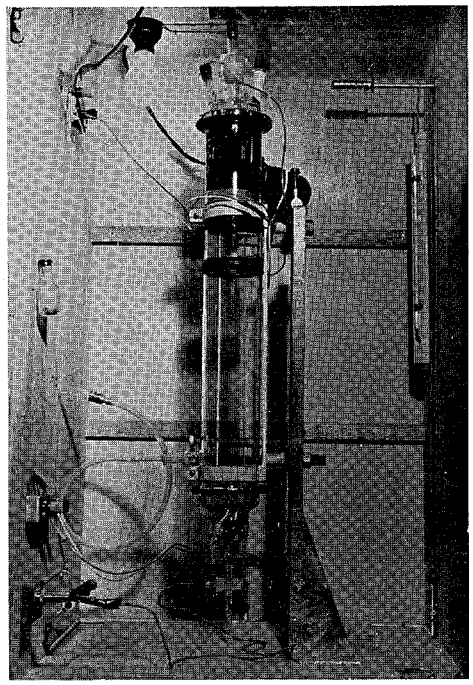

Snow making apparatus

8

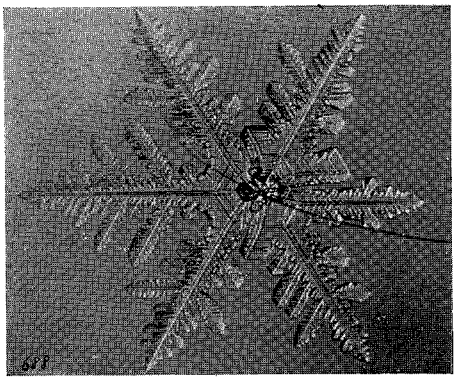

× 26

9

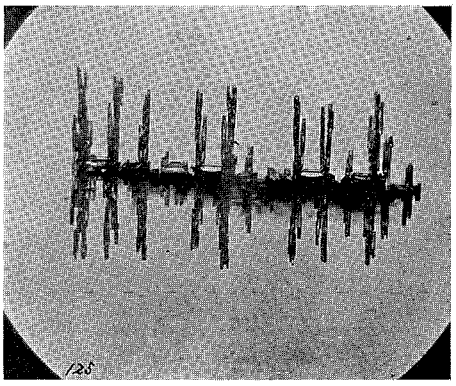

× 10.5

10

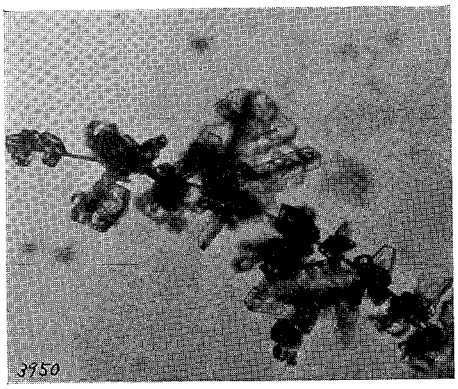

× 47

11

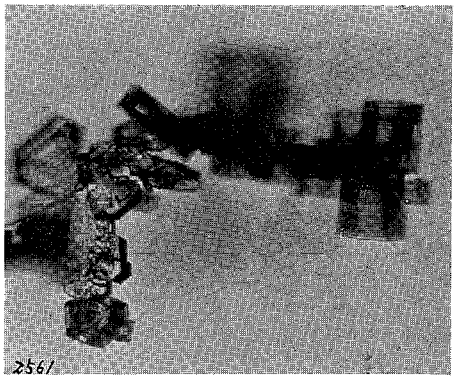

× 26

12

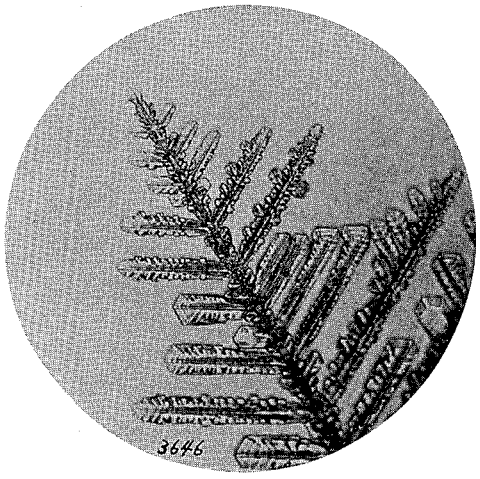

× 54

13

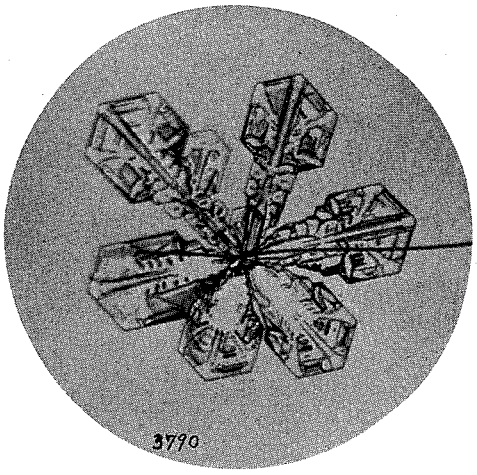

× 31

14

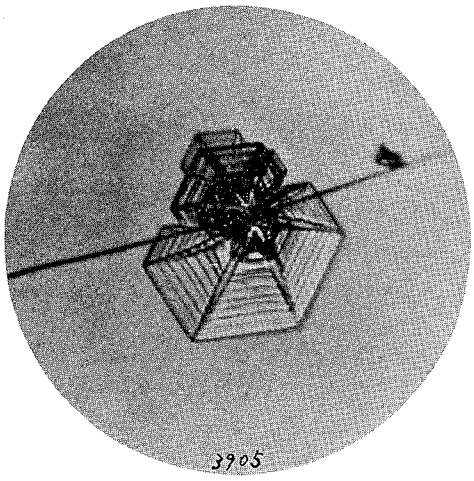

× 43

15

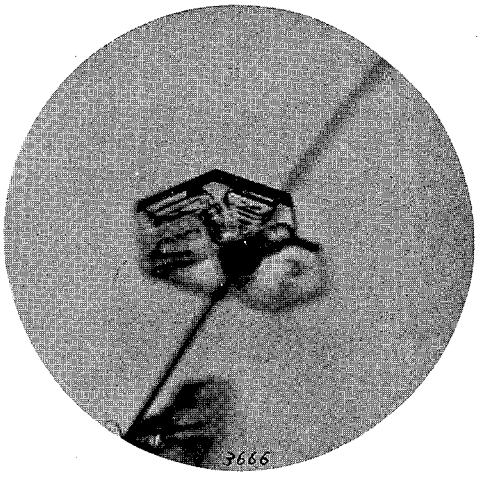

× 42

16

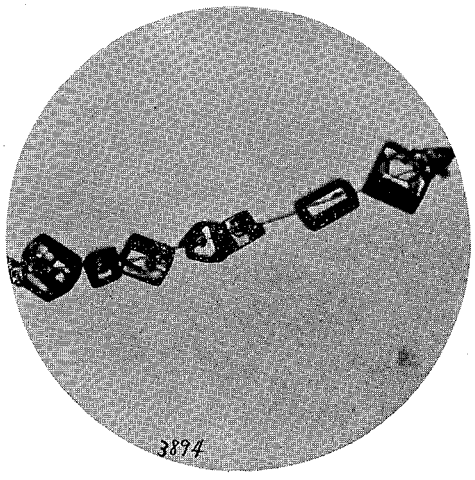

17

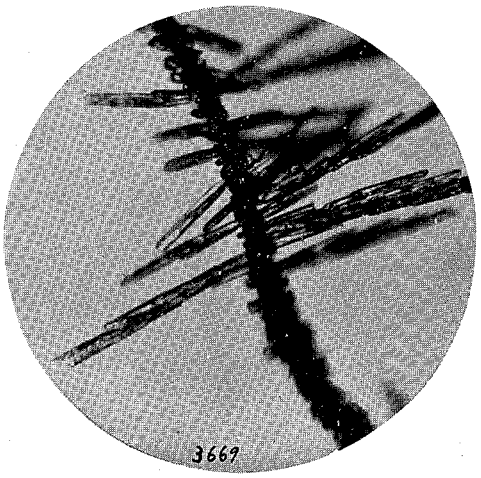

18

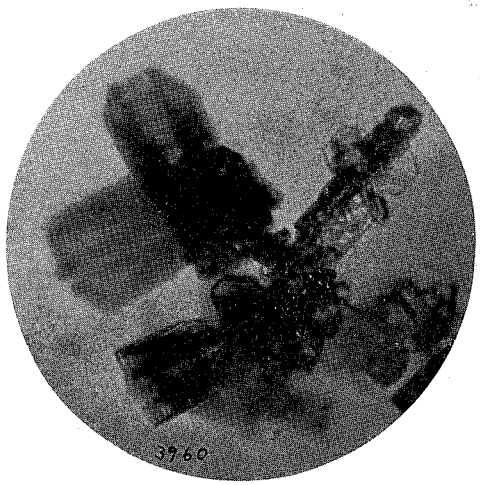

× 57

19

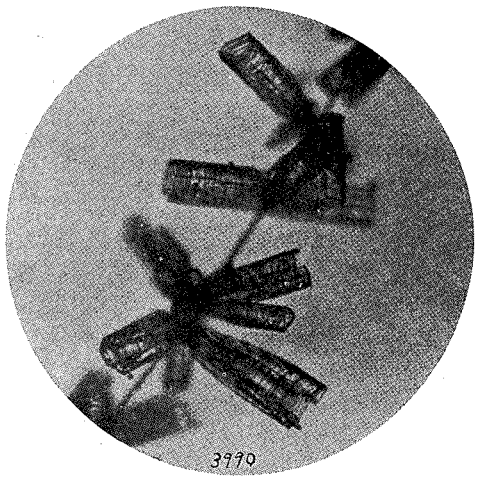

× 54

20

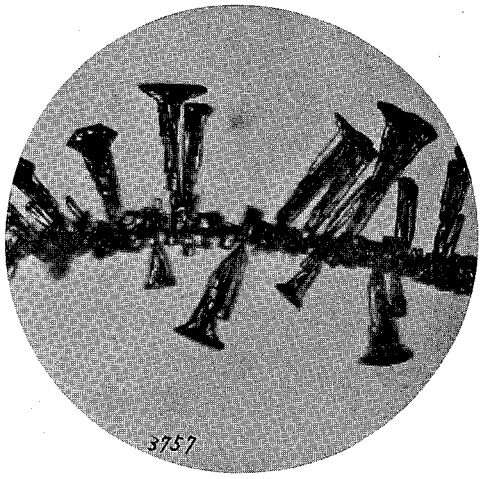

× 31

21

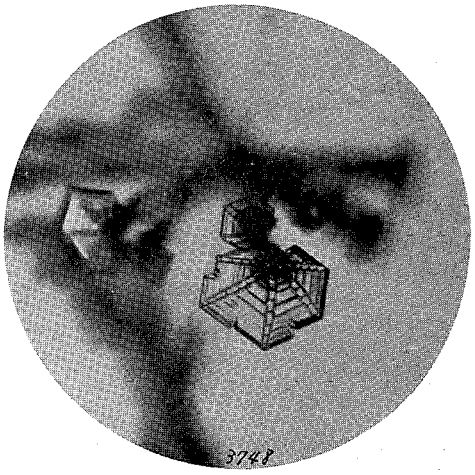

× 37

22

× 31

23

ordinary pin × 9.4

24

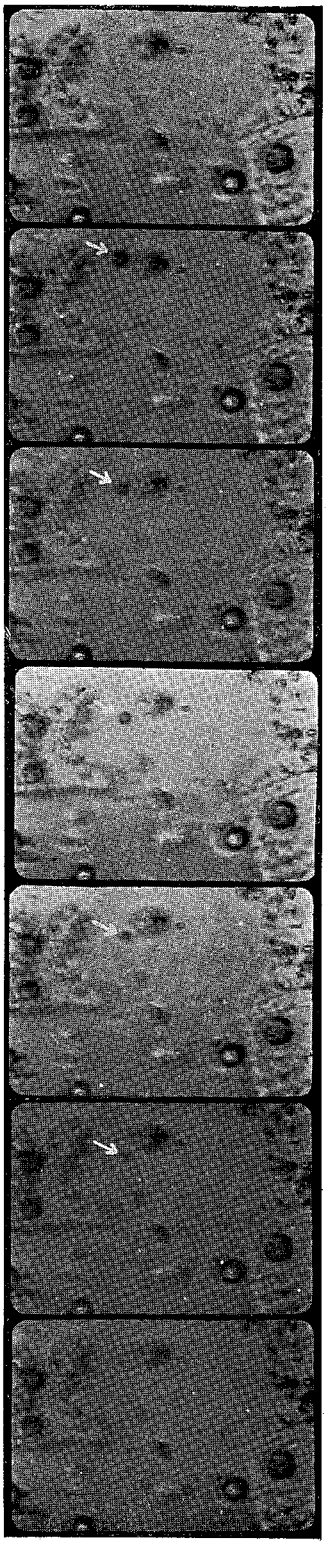

a) $t = 0$

b) 0.05 sec

c) 0.15 sec

d) 0.25 sec

e) 0.35 sec

f) 0.50 sec

g) 0.55 sec

× 420

25

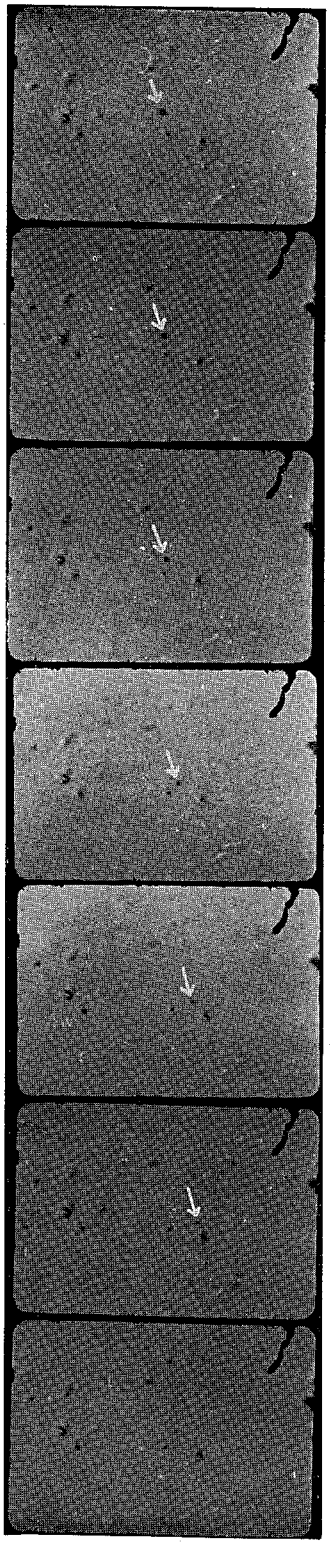

a) $t = 0$

b) 0.05 sec

c) 0.10 sec

d) 0.20 sec

e) 0.30 sec

f) 0.40 sec

g) 0.45 sec

× 203

26

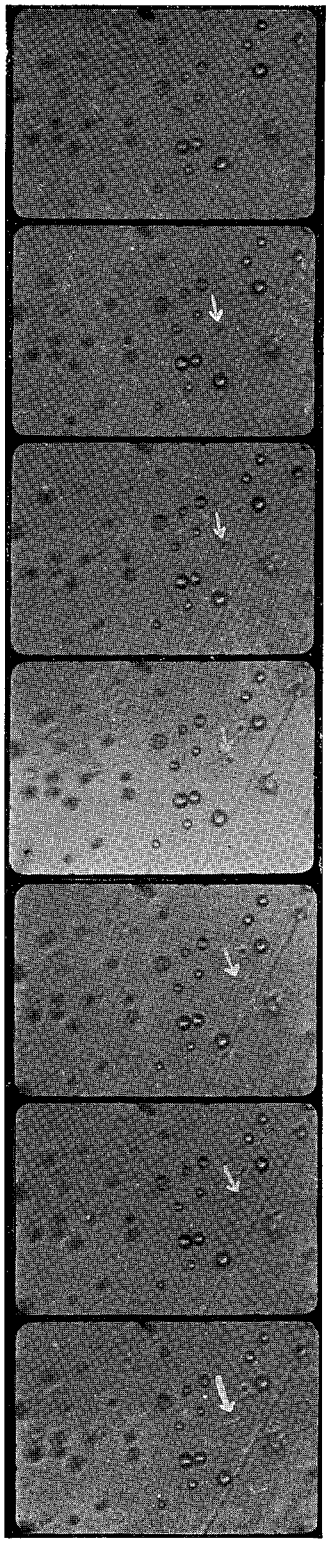

a) $t = 0$

b) 0.05 sec

c) 0.10 sec

d) 0.15 sec

e) 0.25 sec

f) 0.30 sec

g) 0.35 sec

× 203

27

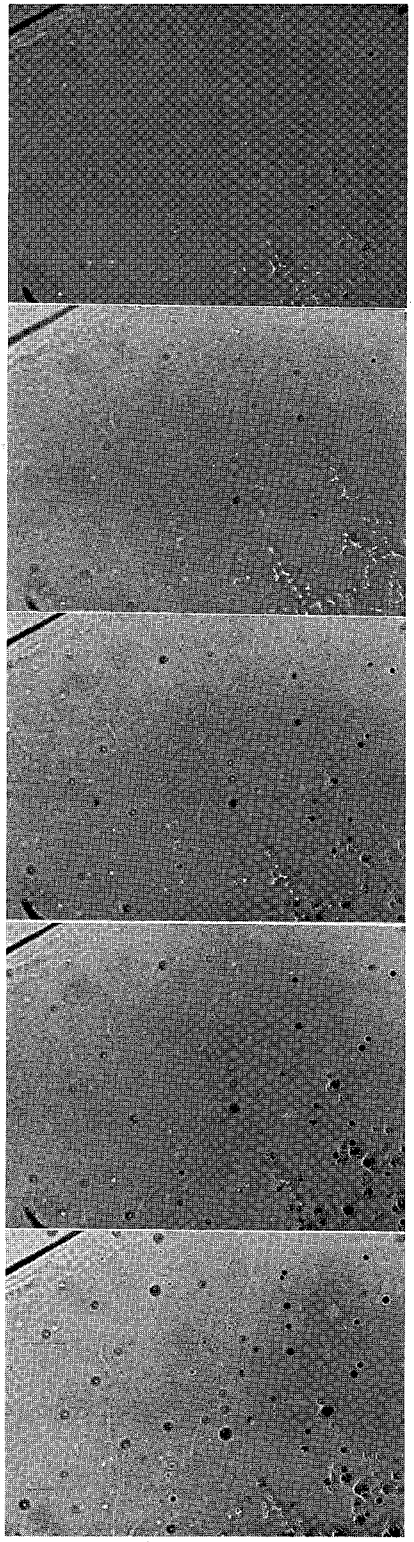

a) $t = 0$

b) 1 min

c) 2 min

d) 3 min

e) 4 min

× 91

28

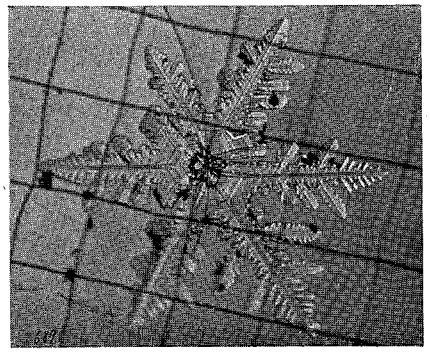

Sample No. 57, $\theta = -25°C$, $t = 0$, × 24

29

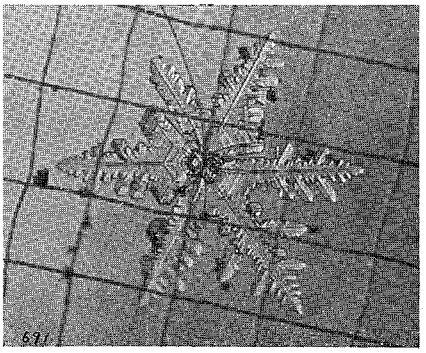

t = 5 m, × 24

30

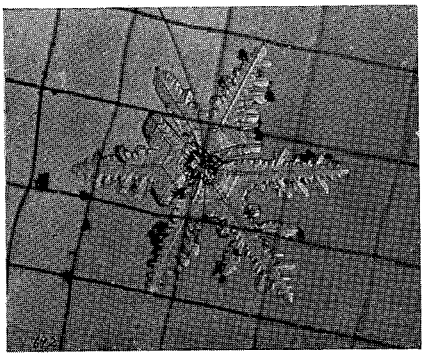

t = 11 m, × 24

31

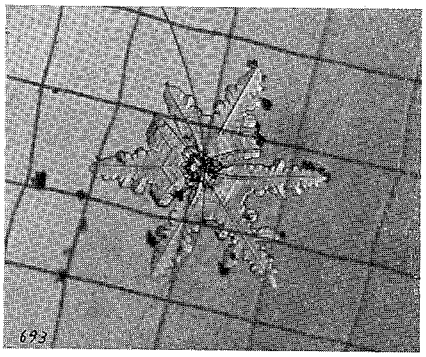

t = 17 m, × 24

32

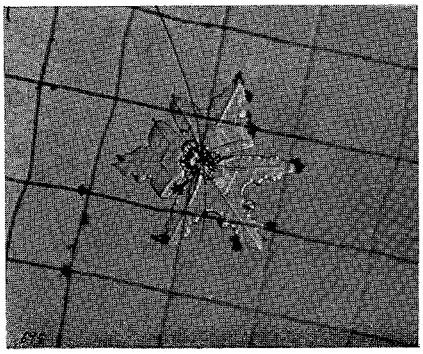

t = 27 m, × 24

33

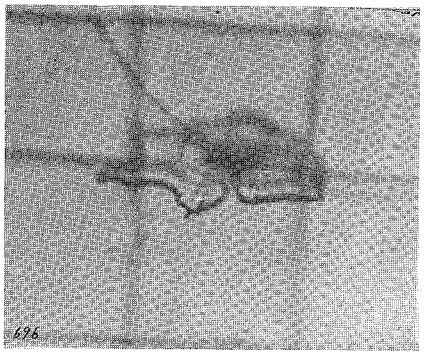

t = 38 m, × 44

34

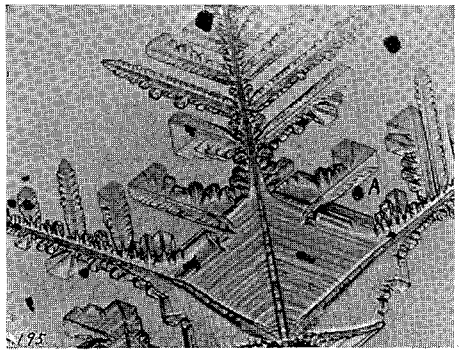

Sample No. 11, $\theta = -4°C$, $t = 0$, × 24

35

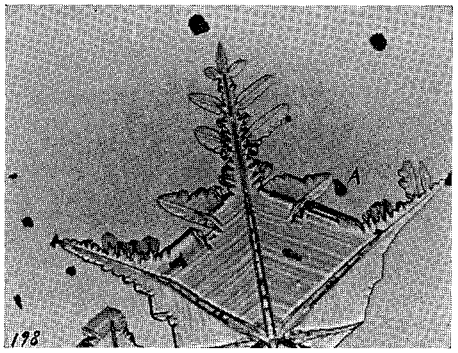

t = 5 m, × 24

36

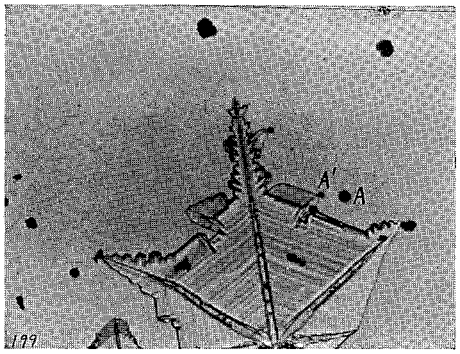

t = 7 m, × 24

37

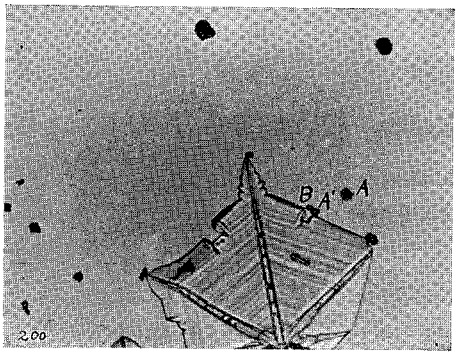

t = 9 m, ×24

38

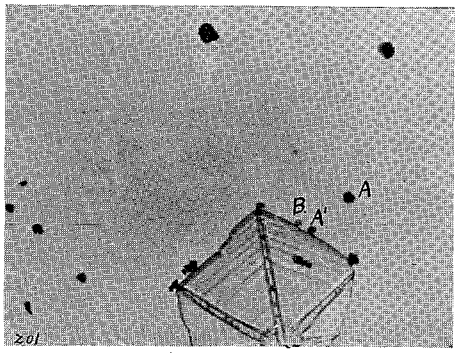

t = 11 m, × 24

39

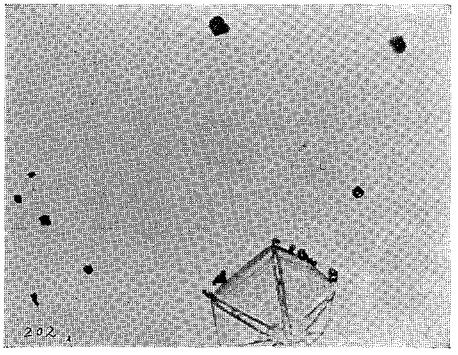

t = 14 m, × 24

40

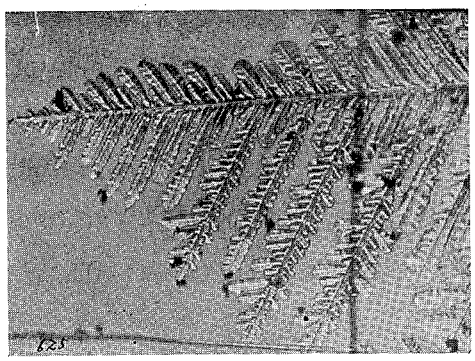

Sample No. 56, $\theta = -28°C$
$\sim -40°C$, $t=0$, × 42

41

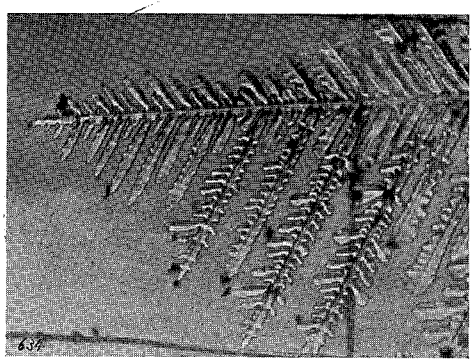

t = 6 h 12 m, × 42

42

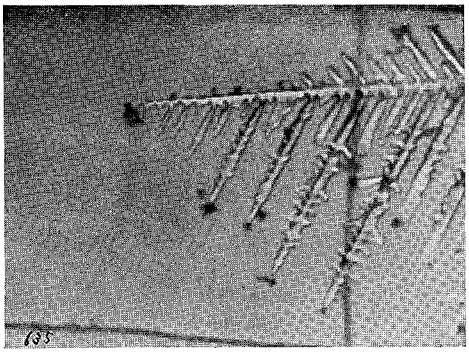

t = 21 h 10 m, × 42

43

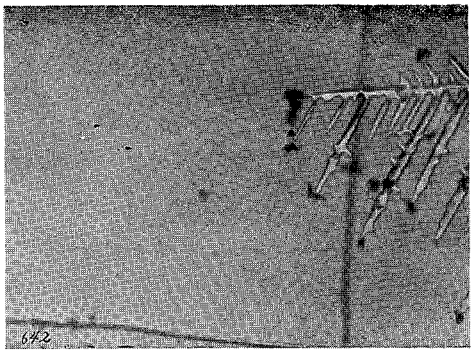

t = 27 h 47 m, × 42

44

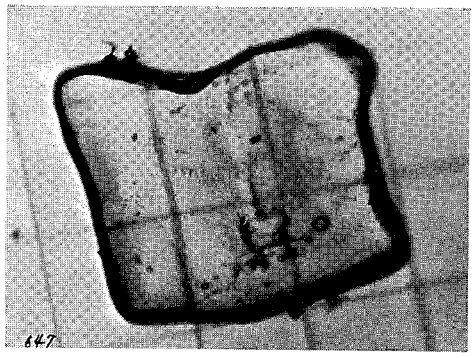

Para-dichlor-benzol,
$\theta = 10°C$, $t=0$, × 38

45

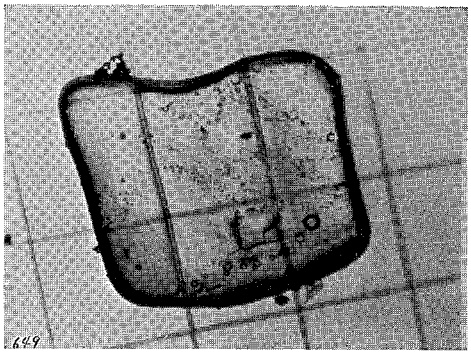

t = 7 m, × 38

46

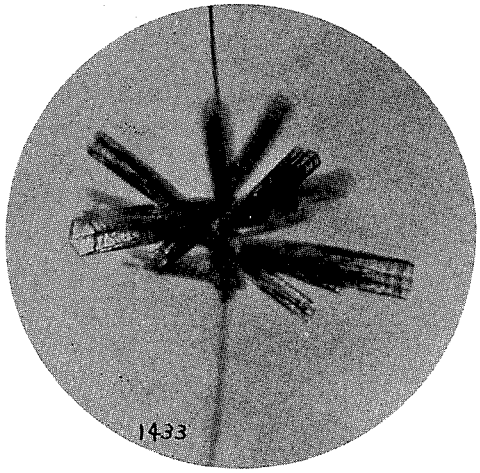

dendritic region, × 31

47

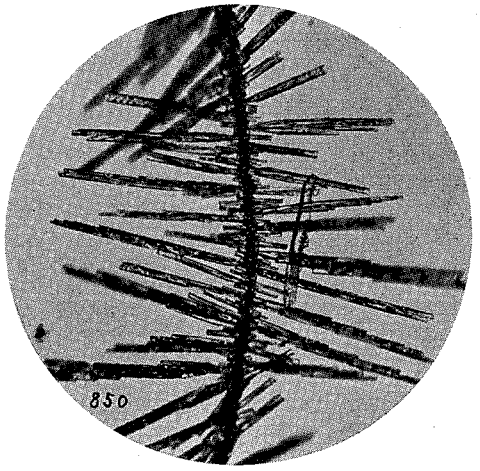

needle region, × 17

48

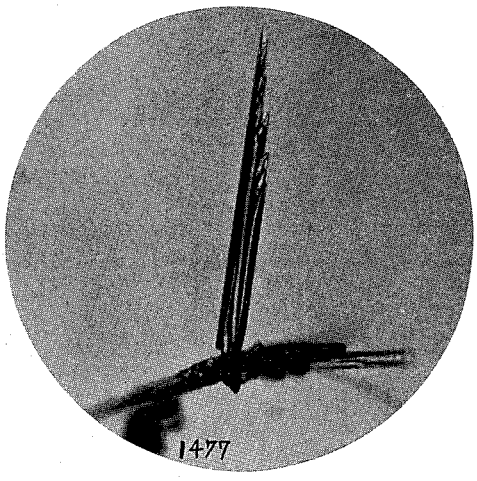

needle region, × 31

49

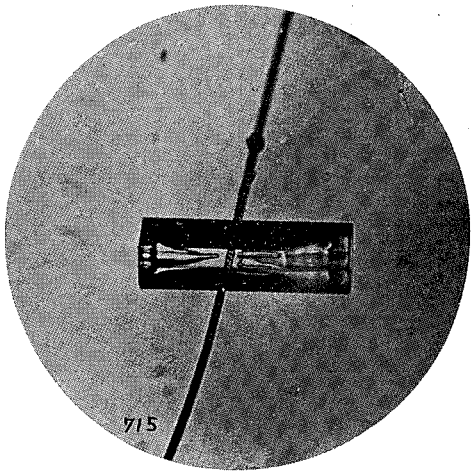

spatial plates region, × 74

50

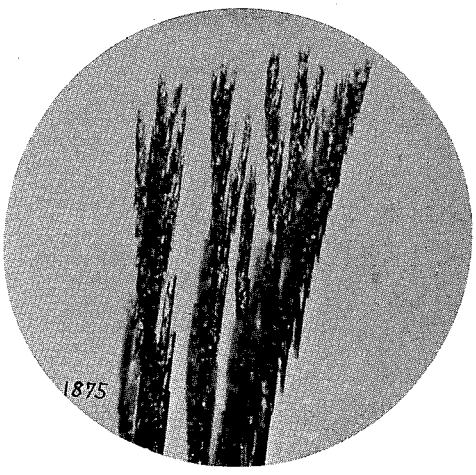

51

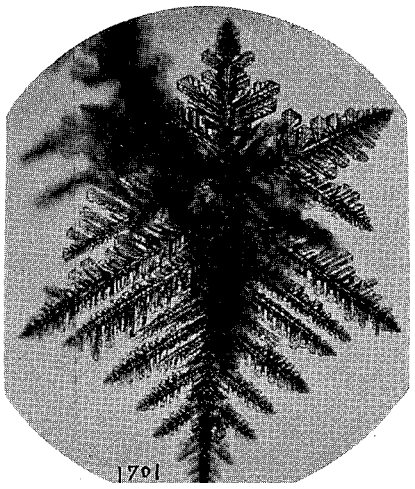

52

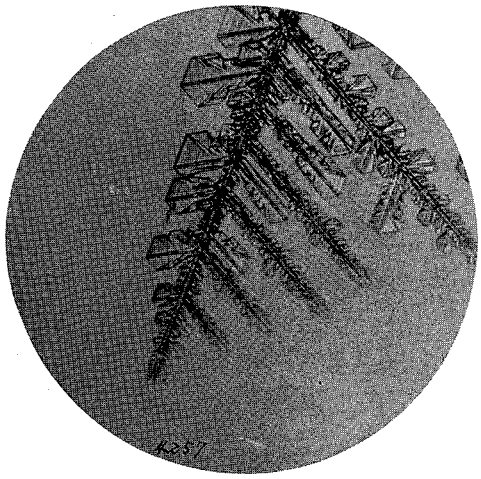

Clean aerosol free air, × 31

53

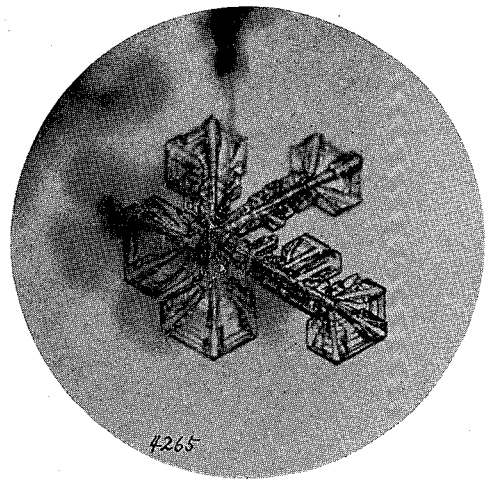

acetone trap $T = -180°C$, × 31

54

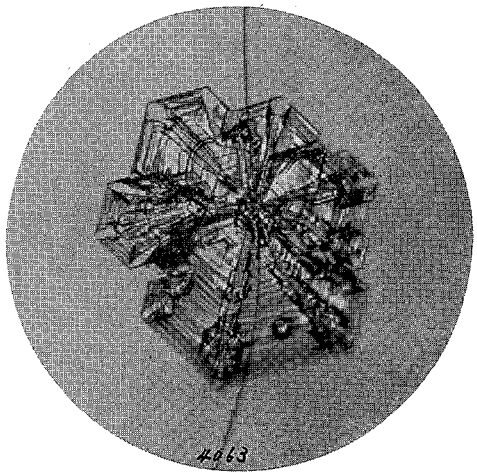

$T = -180°C \sim -74°C$, × 31

55

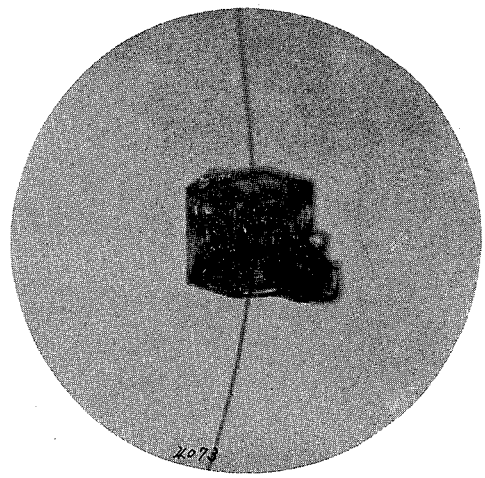

$T = -74°C$, × 33

56

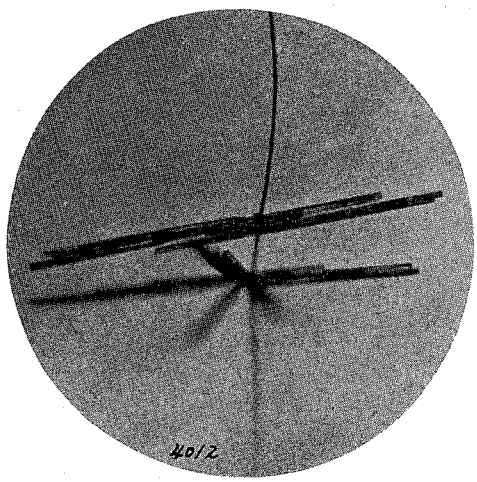

57

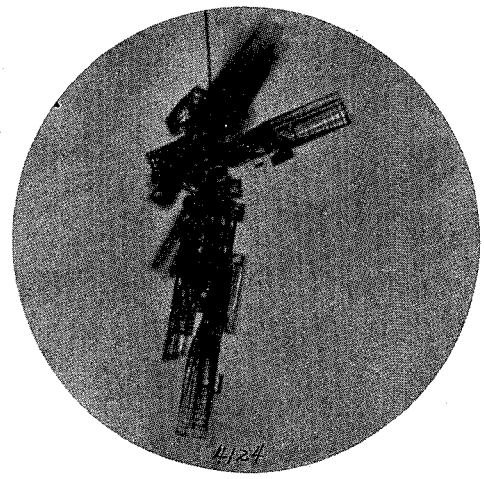

58

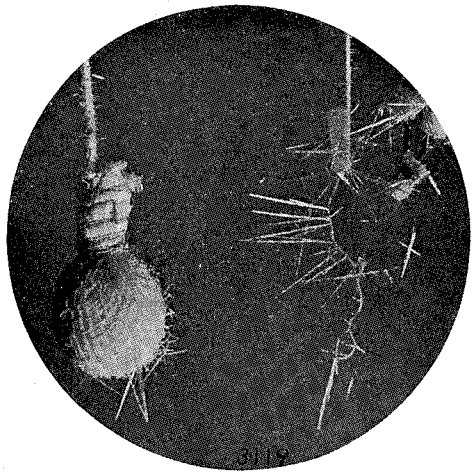

Acetone, × 1.4

59

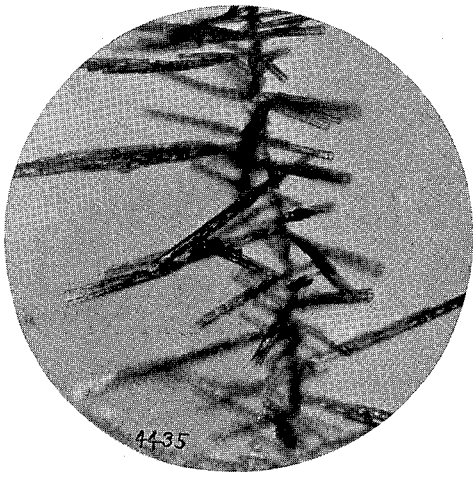

methyl-ethyl-ketone, × 31

60

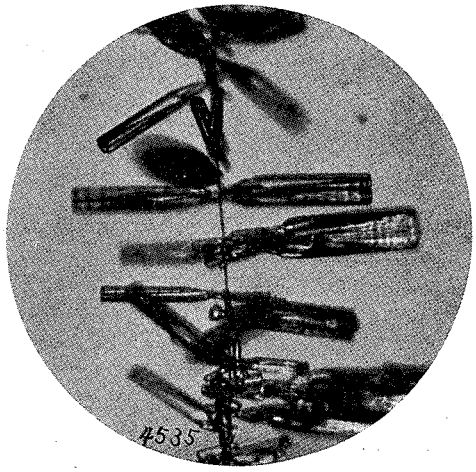

Diethyl oxide, × 33

61

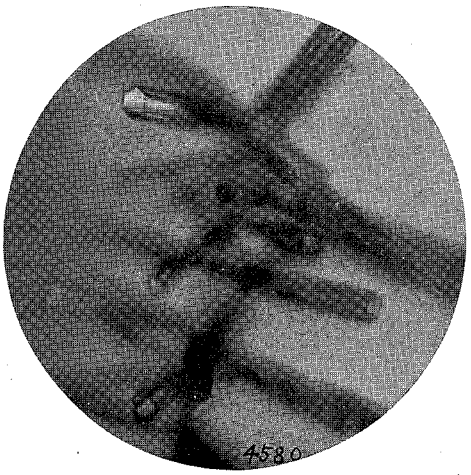

Amyl acetate, × 33

62

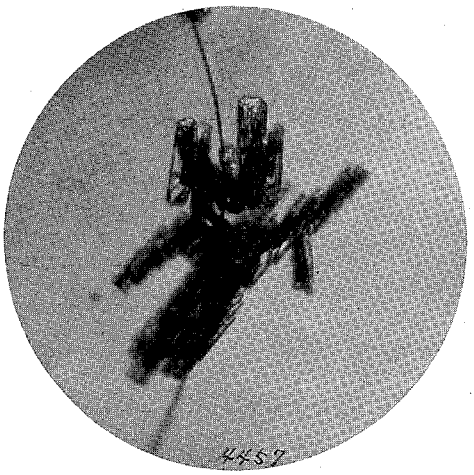

63

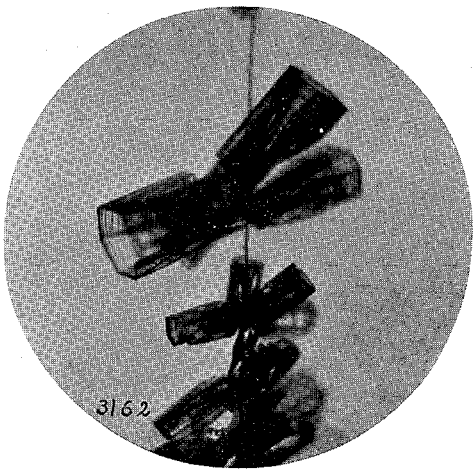

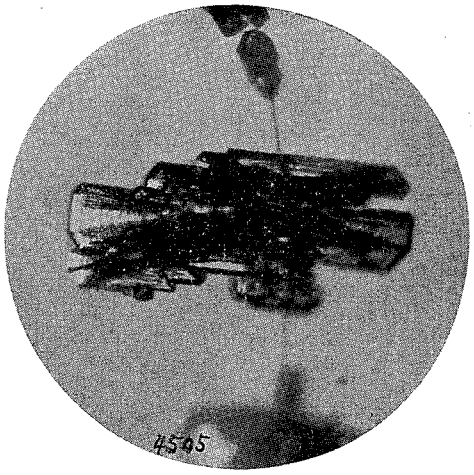

Methylene chloride, × 31

66

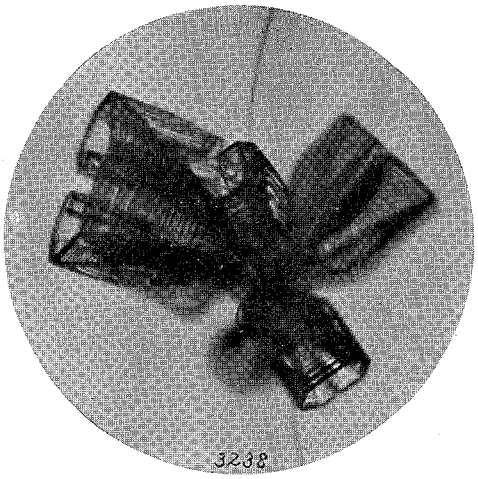

Benzol, × 31

67

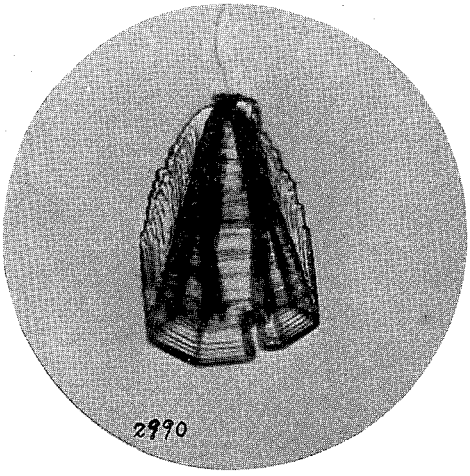

Toluene, × 31

68

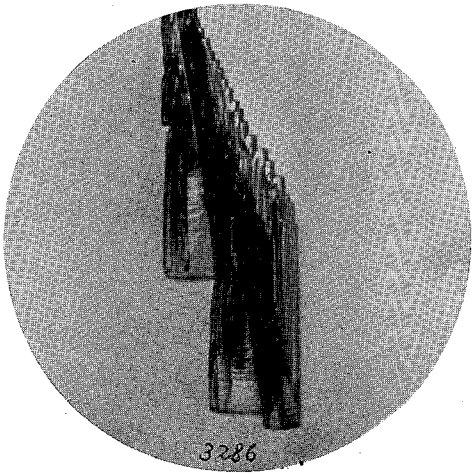

Ether, × 31

69

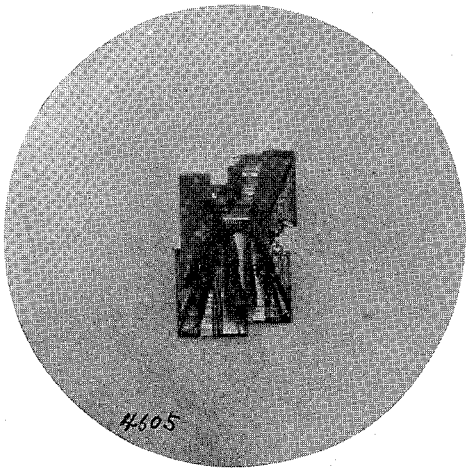

Chloroform × 31

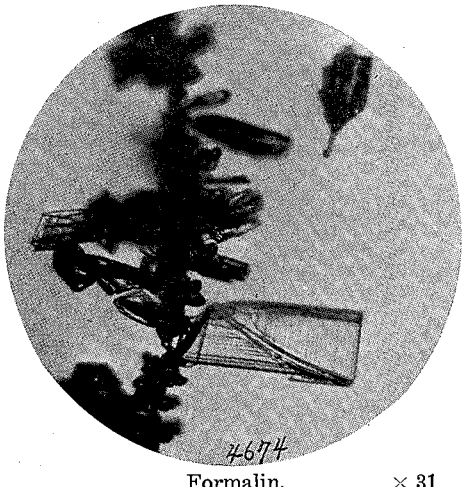

Formalin. × 31

70

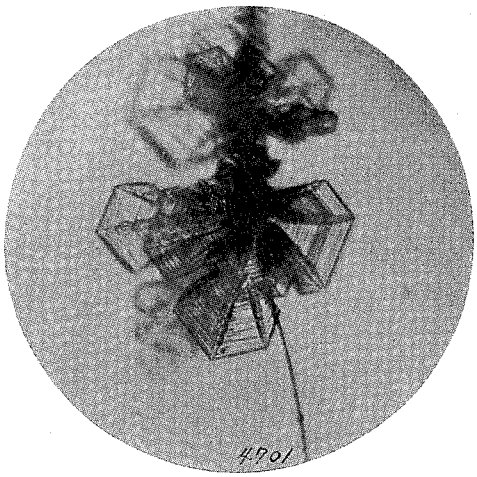

Caprylic acid, × 31

71

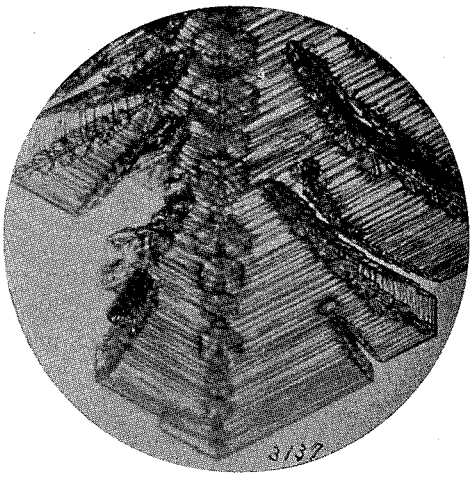

methyl alcohol, × 31

72

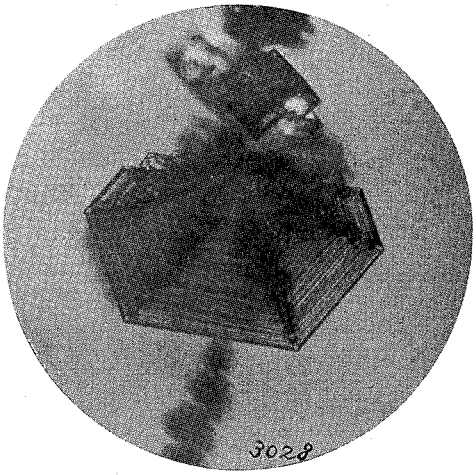

Ethyl alcohol, front view, × 31

73

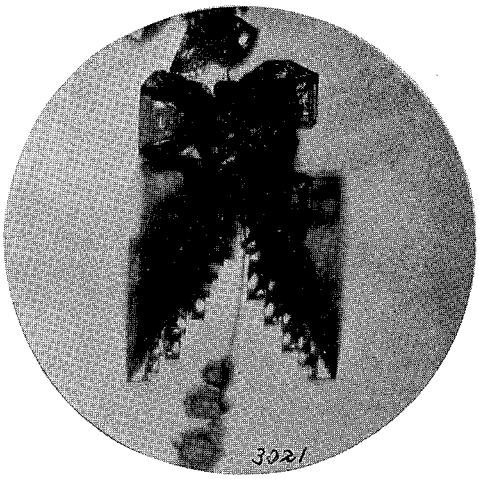

Ethyl alcohol, side view, × 31

74

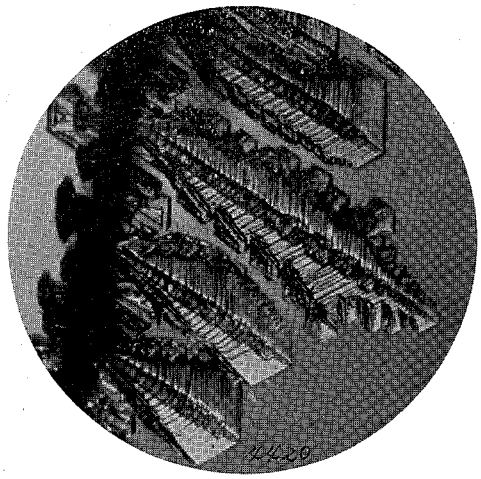

75